EFFECT OF VORTEX GENERATOR ON BLOOD FLOW CHARACTERISTIC ON IDEALIZED PROSTHETIC HEART VALVE

LIM BOON HONG

UNIVERSITI TEKNIKAL MALAYSIA MELAKA

EFFECT OF VORTEX GENERATOR ON BLOOD FLOW CHARACTERISTIC ON IDEALIZED PROSTHETIC HEART VALVE

LIM BOON HONG

This report is submitted
in fulfillment of the requirement for the degree of
Bachelor of Mechanical Engineering

Faculty of Mechanical Engineering

UNIVERSITI TEKNIKAL MALAYSIA MELAKA

JUNE 2020

DECLARATION

I declare that this project report entitled “ Effect of Vortex Generator on Blood Flow Characteristic on Idealized Prosthetic Heart Valve” is the result of my own work except as cited in the references

Signature : ....

Name : ....

Date : ....

APPROVAL

I hereby declare that I have read this project report and in my opinion this report is sufficient in terms of scope and quality for the award of the degree of Bachelor of Mechanical Engineering.

Signature :. ....

Name of Supervisor : ....

Date : ....

DEDICATION

To my beloved mother and father

ABSTRACT

Bi-leaflet Mechanical Heart Valve (BMHV) is widely used in surgically heart valve replacement in worldwide. The main complication of the BMHV is that BMHV leaded to the formation of blood clotting known as thrombosis. Vortex Generator (VG) is used to improve the performance of the BMHV by delaying the turbulence that activated the platelet and hemolysis. This paper presents various configuration of VG to enhance the performance of BMHV. In this Computational Fluid Dynamic (CFD) simulation, a simplified prosthetic heart valve is used to investigate the performance of BMHV with different orientation of VG. As a result, the fluid is passed through the leaflets with VG. The pressure drop is decreased between the position of after leaflets and before leaflets. In the present study, four different configurations of VG are reviewed, which are without VG, Co-counter Equally Spaced VG, Straight Equally Spaced VG and Counter-rotating Far Spaced VG. In the other hand, this present study also investigates the pulsatile turbulent transient flow in simplified prosthetic heart valve with no VG and the best configuration of VG in the previous study. In the present study, Co-counter Equally Spaced VG is the best configuration and it contributed 42.62% of improvement in pressure drop across the leaflets. Besides that, Co-counter Equally Spaced provided 52.96% and 7.82% reduction in Turbulence Shear Stress and Turbulence Kinetic Energy respectively. In the summary, the pressure drop, turbulence kinetic energy and turbulence shear stress are significantly reduced due to the existence of VG. VG is a crucial device to enhance the performance of BMHV by delaying early separation and thus turbulence reduced.

ABSTRAK

Bi-leaflet Mechanical Heart Valve (BMHV) digunakan dalam penggantian injap jantung pembedahan di seluruh dunia. Terdapat masalah yang serius dengan penggunaan peralatan ini adalah peralatan ini boleh membawa kepada pembentukan pembekuan darah dalam jantung kita. Vortex Generator (VG) adalah peranti yang dapat digunakan untuk menambahbaikkan prestasi BMHV. VG dapat melambatkan pergolakan dalam aliran darah di jantung. Projek ini dijalankan untuk menyiasatkan beberapa konfigurasi VG untuk meningkatkan prestasi BMHV. Dalam Computational Fluid Dynamic (CFD) simulasi, satu prostetik injap jantung digunakan untuk menyiasatkan prestasi BMHV dalam konfigurasi VG yang berbeza. Darah disimulasikan dalam injap jantung prostetik tersebut yang mempunyai pemasangan VG. Dalam simulasi ini, hasilnya dijankakan tekanan dapat dikurangkan selepas pemasangan VG di dalam prostetik injap jantung Terdapat empat konfigurasi yang berbeza dalam projek ini iaitu kes yang tidak mempunyai VG, Co-counter Equally Spaced VG, Straight Equally Spaced VG dan Counter-rotating Far Spaced VG. Selain itu, projek ini juga menjalankan penyiasatkan aliran pendenyutan dalam prostetik injap jantung. Perbandingan juga dilaksanakan antara kes yang tidak mempunyai VG and konfigurasi VG yang terbaik. Dalam projek ini, Co-counter Equally Spaced ialah konfugurasi yang terbaik dalam perbandingan beberapa reka cipta yang lain. Terdapat 42.62% pengurangan tekanan dengan penggunaan konfigurasi Co-counter Equally Spaced VG. Selain itu, Co-counter Equally Spaced VG dapat menambahbaikkan tenaga kinetik tubulensi dan tekanan tubulensi sebanyak 52.96% dan 7.82%. Konklusinya, VG dapat mengurangkan tekanan dan tenaga kinetik pergolakan dengan berkesan. VG adalah sesuatu peralatan yang sangat penting dalam penambahbaikan prestasi BMHV.

ACKNOWLEDGEMENT

It was an excellent opportunity to be able to have final year project related to bio-mechanical engineering during my final year period. I gained abundance of hands on experiences and knowledge. I am glad to meet many individuals and keen parties who had guided me through execution of project work.

Firstly, I would like to take this opportunity to express my gratitude to my supervisor, Dr. Mohamad Shukri bin Zakaria from Faculty of Mechanical Engineering, University Teknikal Malaysia Melaka (UTeM) for his altruistically teachings and support towards my project.

I would also like to express my deepest sense of gratitude to my Computational Fluid Mechanic lecturer, Dr. Suhaimi bin Misha from Faculty of Mechanical Engineering for his precious guidance of CFD simulation in my project work. Furthermore, I would like to express my profound gratitude to my peers who helped me in the critical situation during my project work.

Finally, I would also like to express my special thanks to my family and siblings for their impartial and selfless moral support. Without them, this project work would not be able to finish in time. I am thankful to all the people who involved in my project work, and I am lucky enough to have such encouragement, guidance, and support from them.

I will cherish this opportunity as a steppingstone for my future career's development. I will strive to achieve my desired career objectives with the skills and knowledge learnt.

CONTENT

LIST OF FIGURES

LIST OF TABLES

LIST OF SYMBOLS

α	-	Angle of Attack
λ	-	Wavelength between two VG
C_d	-	Drag Coefficient
U_o	-	Velocity of Flow
S_{min}	-	Minimum spacing between two VG
Re	-	Reynolds number
ρ	-	Density
V	-	Mean Velocity
D	-	Diameter of tube
μ	-	Dynamic Viscosity
ν	-	Kinematic Viscosity
W_n	-	Womersley number
ω	-	Angular Velocity
P	-	Pressure
I	-	Turbulence Intensity
C_μ	-	Turbulence Model Contact
l	-	Turbulence Length Scale
η	-	Eddy Viscosity

LIST OF ABBREVIATION

SJM	-	St. Jude Medical
RBC	-	Red Blood Cell
BHV	-	Bioprosthetic Heart Valve
MHV	-	Mechanical Heart Valve
BMHV	-	Bi-leaflet Mechanical Heart Valve
VG	-	Vortex Generator
EOA	-	Effective Orifice Area
CFD	-	Computational Fluid Dynamic
UDF	-	User-Defined Function
RHS	-	Right Hand Side
LHS	-	Left Hand Side
TKE	-	Turbulence Kinetic Energy
RSS	-	Reynolds Shear Stress

CHAPTER 1

INTRODUCTION

1.1 Background

Heart failure is a life-threatening illness and it indicated that a current worldwide wellbeing priority. Approximately 26 million people worldwide are living with heart failure (Ponikowski *et al.*, 2014). The heart diseases are included coronary artery disease, transplants and ventricular assist devices (VADs) for heart failure congestion or valve replacement (James, Papavassiliou and O'Rear, 2019).

The general structure of the heart is shown in Figure 1.1 below. Heart valve is used to provide unidirectional blood flow through the heart (Sotiropoulos, Le and Gilmanov, 2016). The heart valve failure happened when the valve does not close completely, caused the blood to start to flow backward. This condition occurred will lead to the heart started to pump harder and became less efficient. In heart valve disease treatment, patients have 2 main treatment options which are heart valve repair and replacement. For the first option, the patients can keep their valve and leaflets but only used for mitral and tricuspid valve regurgitation. Besides that, valve replacement required a new valve to be inserted surgically in the heart.

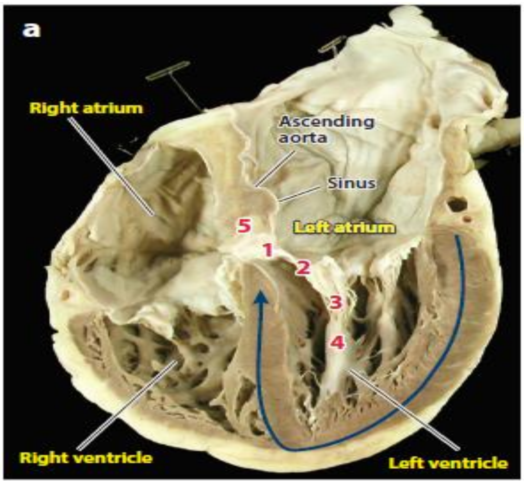

Figure 1.1: Anatomy of the human heart (Sotiropoulos, Le and Gilmanov, 2016)**.**

According to the Department of Statistics Malaysia, Ischaemic heart disease is the highest causes of death facing by Malaysians in the last year 2018. About 15.6% of Malaysian are suffering from the Ischaemic heart diseases as shown in Figure 1.2 below. Ischaemic heart diseases also known as coronary heart diseases. The waxy substances inside the coronary arteries is a factor to cause Ischaemic heart diseases. These waxy substances are partially or totally block the blood flow through the heart. Many Malaysians do not notice that they suffer from ischaemic heart disease until they experience some complications such as heart attack (*Ischemic Heart Disease | National Heart, Lung, and Blood Institute (NHLBI)*, no date).

In the category of Ischaemic heart diseases, a total of 12,510 men is suffered Ischaemic heart diseases. It showed that the men have higher chances to get diseases compared to women which are about 36.97%. From the perspective of races, the Bumiputera has contributed the highest total of amount (11,350 of people) who are suffering from the Ischaemic heart diseases followed by Chinese (4,243 of people) and Indian (2,240 of people). The average of causes of death for Ischaemic heart diseases is about 50 persons per day in Malaysia. On the other hand, the principal causes of death for Ischaemic heart diseases are mostly in the age of 60 years and above. It means that the golden ages of people have larger chances to have Ischaemic heart diseases.

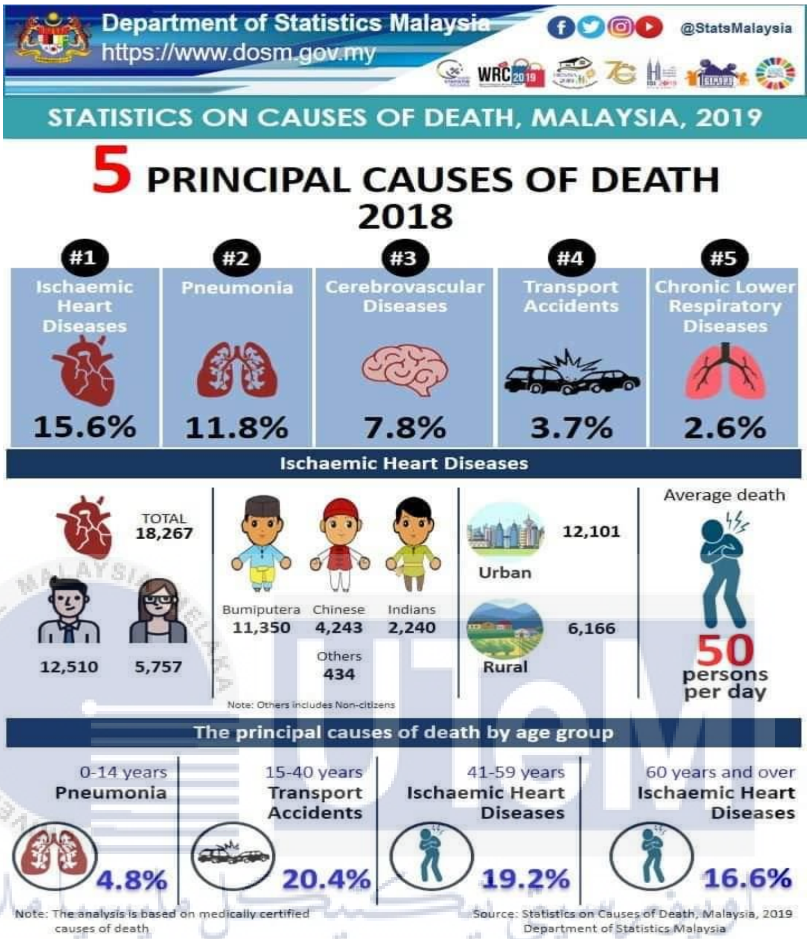

Figure 1.2: Statistics on Causes of Death in Malaysia, 2019.

The prosthetic heart valve is commonly surgically implanted for the occurrence of valvular heart disease. In current existing commercial, the prosthetic heart valve is divided into 2 major type which is the mechanical heart valve and bioprosthetic heart valve. Over 300000 heart surgical heart valve replacement operation is carried out worldwide annually, where 40~60% of the operations are using bioprosthetic heart valve produced by using glutaraldehyde-fixed animal tissues. The advantages of implantation of bioprosthetic heart valve are durable, particularly in older patients for more than 60 years old (Li, 2019). Second, it does not have thrombosis complication. The most crucial point is that the bioprosthetic heart valve does not last long and has a shorter life span of about 7 to 10 years compared to a mechanical heart valve. On the other hand, high durability is the main advantage of mechanical heart valve. The mechanical heart valve can last throughout the entire life cycle of the patient. But the main complication of mechanical heart valve is the formation of blood clotting known as thrombosis (Zakaria *et al.*, 2017).

Both Zakaria et al. (2017) and Hatoum and Dasi (2019) stated that tremendous progress has been made in the development of MHVs over the past 60 years to improve their stability and performance in reducing complications of blood clotting. There are several types of design in MHV's family which are shown in Figure 1.3. In this study, St. Jude Medical (SJM) mechanical heart valve was selected to investigate the impact of turbulent flow in this idealized geometry design. Computational simulation of flow through idealized mechanical heart valve is included in this study. Turbulent flow are well-established factors that contribute to the hemolysis of the valve and the activation of platelets. Consequently, any new mechanical heart valve design aims to minimize the risk of activation of platelets and hemolysis by increasing the turbulent pressure (Hatoum *et al.*, 2018). To achieve the goals, a vortex generator installed with an ideal configuration in an idealized mechanical valve is investigated in this study.

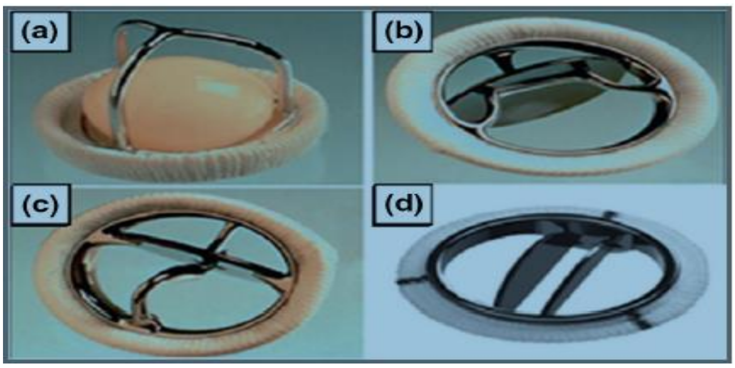

Figure 1.3: (a) Caged ball valve (b) Bjork-Shiley tilting disk valve (c) Medtronic Hall tilting disk valve (d) St. Jude Medical Regent bileaflet valve. (Zakaria *et al.*, 2017).

Figure 1.4: Bioprosthetic heart valve (Pibarot and Dumesnil, 2009).

1.2 Problem Statement

Artificial heart valve can expose blood to flow that condition in unnaturally high blood cell pressure and damage as well as thrombosis (James, Papavassiliou and O'Rear, 2019). For current main concern is that the installation of foreign objects which is either a mechanical heart valve or bioprosthetic heart valve may lead to the blood flow in unnatural condition. According to the research of Hund, Antaki and Massoudi (2010), it stated that foreign objects such as artificial heart valves are generated turbulent flow. The turbulent stress of non-physiological flow is harm to the RBC and platelets. This will lead to the occurrence of blood clotting. Besides that, a high-speed leakage jet experienced high shear stresses, separation of flow to increase the formation of blood clots (Zakaria *et al.*, 2017).

Despite strong anticoagulation treatment, thromboembolism is the most common complication linked with mechanical heart valves. Around 0.1-5.7 percent per patient per year (Hatoum and Dasi, 2019). Clinical studies found that patients with mechanical valves had been reduced half-lives of RBC and platelets. However, given the potential for thromboembolism complications, mechanical heart valve recipients must take anticoagulant medication. Such complication are believed to cause high blood shear stress, turbulent flow and overall difficulty of hemodynamic in the mechanical heart valve (Ge *et al.*, 2003).

Besides that, the mechanical heart valve without the vortex generator may increase the risk of thrombosis. Hatoum and Dasi (2019) stated that the presence of vortex generators removes the inflection point indicating the direction of the boundary layer separation. This indicated that the separation has reduced significantly. Downstream pressure recovery is significantly improved when separation and recirculation is decreased.

1.3 Objective of Project

The main objective of research is to reduce the formation of blood clotting and thrombosis in terms of reducing the pressure gradient and shear stress in bi-leaflet mechanical heart valve. Hence, the specific aims are:

a) To investigate the effect of turbulent flow in an idealized prosthetic heart valve.
b) To analyze the effect of vortex generator on blood flow in an idealized prosthetic heart valve.

1.4 Scope of Project

The scopes of present study as followed below:

a) Using numerical simulation only. (ANSYS Workbench 16.1)
b) 3D geometry of aorta. (Idealized Geometry)
c) Laminar flow and Turbulent flow inside the aorta.
d) St. Jude Medical Standard of Mechanical Heart Valve.
e) Leaflets are placed 5° to the horizontal. (Fully Opened)
f) Turbulence model k-ε is used.

CHAPTER 2

LITERATURE REVIEW

This chapter introduces the theories and related scientific knowledge in this research topic. Previous works related to this research were reviewed to obtain ideas and references for current work.

2.1 Mechanical Heart Valve

In this era modern world, prosthetic system substitution remains a major therapy option for heart disease patient. Although bioprosthetic heart valve (BHV) remains the most common replacement heart valve in the medical field, its durability still limited. This is, therefore, an ongoing requires to establish a general understanding of the mechanisms that restrict BHV durability to facilitate the production of a more durable prosthetic (Zakerzadeh, Hsu and Sacks, 2017). In this regard, a mechanical heart valve (MHV) is introduced and to overcome the BHV complications. On the other hand, MHV has its complications. In recipients of MHV, thrombus development is a major concern which allows them to take anticoagulant medicine for the rest of their life (Hedayat, Asgharzadeh and Borazjani, 2017). Many patients required to take anticoagulants for the entire life after MHV has been installed. Anticoagulant is used to slow down the formation of thrombus, preventing complications on the artificial valve. If the anticoagulant drugs ignored by recipients, it would enhance the valve obstruction and causing a stroke.

BHV has a shorter life span (10-15 years) than MHV (entire life), whereas MHV is less biocompatible and vigorously rejected by human body. The foreign object exposed to the blood; a turbulent flow condition can be generated. In a high shear stress condition, the activation of platelets is increased. Hemolysis due to prosthetic heart valve has been discussed since the 1960s (James, Papavassiliou and O'Rear, 2019).

Choosing a substitute for MHV or BHV is a significant decision, affected by the interchanges between potential need for reaction due to BHV degradation and the risk correlated with anticoagulation in long term for MHV (Zakerzadeh, Hsu and Sacks, 2017). The current design of bi-leaflet valve is significantly different from the natural valve. Compared to the natural heart valve, the flow field is completely different in the bi-leaflet valve. In previous study, it showed that the heart valve design is a crucial impact on the aortic flow area (Akutsu and Matsumoto, 2010). According to Hatoum and Dasi (2019), St. Jude Medical (SJM) mechanical valve as shown in Figure 2.1 below, well known for its excellent hemodynamic quality and low relative thrombogenicity. The layout design valve of SJM is made up of two semi-circular leaflets pivoting on hinges. This provides a good central flow relative to other mechanical valve prostheses such as ball and cage, and the pressure drop across the valve is negligible (Mohammadi, Jahandardoost and Fradet, 2015).

Figure 2.1: SJM Bi-leaflet Mechanical Heart Valve.

2.2 Hemodynamic Blood Clot

While MHV can last longer than BHV, but MBV may cause some complication such as cavitation and intermittent regurgitation. Cavitation occurred when the pressure at a localized area is suddenly decreased as the blood passes through. When the pressure drops under the vapor pressure of blood, some of the blood cell are vaporized into bubbles. This will lead to the blood cell to burst in spots along the flow of blood where pressure is increased. The bursting bubbles distributed energy instantly affect the valve and its ring. It will generate the cracks and erosion of material.

In intermittent regurgitation, the lack of harmonization of leaflets can reduce cardiac output. As the valve is closing, the distance between the leaflets and the outer ring is narrowed. The extrusion flow which is high-speed jet flow is producing when the gap is narrowing. The extrusion flow decreased the pressure and cavitation occurred. As pulsatile rate increased, the closing of leaflet also increased. This is lead to an immediate peak extrusion flow rate that triggering cavitation. The leakage of blood flows back to the left ventricle is caused by intermittent regurgitation, which must do more work than a regular situation. Hence, it is causing some complication in patients (Chou *et al.*, 2016).

Besides that, high shear stress also can stimulate the platelet activation, and further promoting thromboembolic complications. According to Bark et al. (2017), BMHV with superhydrophobic coating is found that cell adhesion is reduced dramatically when contact with blood. It indicated that blood material interaction is a key for reduction in thrombotic potential. Furthermore, the coating impacts valve hemodynamics is very small. Therefore, the blood cell damage is reducing due to the blood flow stress. These results indicated that the superhydrophobic coating is one of the potentials may reduce the thromboembolic complication for current issues.

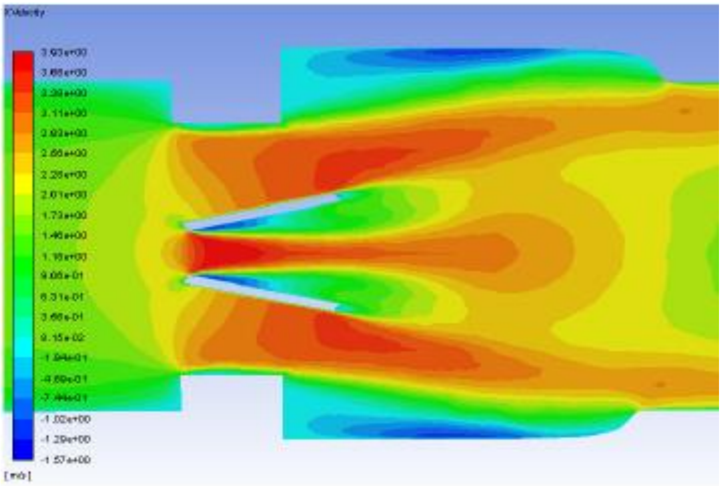

Figure 2.2: Axial Velocity Contour for functioning valve with 1.25m/s blood inlet velocity (James, Papavassiliou and O’Rear, 2019).

The axial velocity contour in a functioning valve with an inlet flow velocity of 1.25m/s is shown in Figure 2.2 above. Orange and red color indicated the peak streamwise velocity around the leaflets. Blue color showed that the backflow and circulation along the inner edge of leaflets and the wall boundary. It showed that it has potential to cause some complication in BMHV.

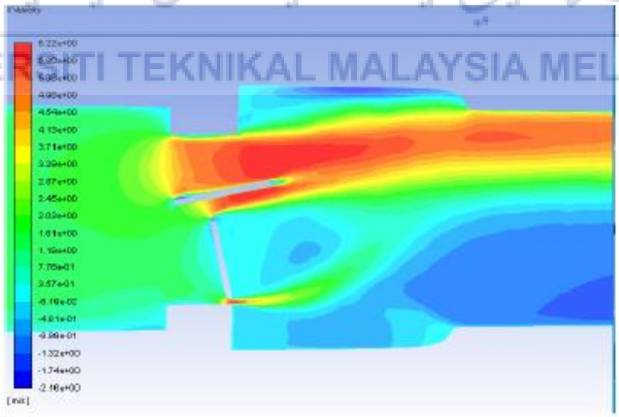

Figure 2.3: Velocity Contour for malfunctioning valve with 1.25m/s blood inlet velocity (James, Papavassiliou and O’Rear, 2019).

The Figure 2.3 showed that the functioning valve of the velocity contour is almost like Figure 2.2**,** but the contour is not symmetric about the centreline. There is a much larger area of backflow and circulation near leaflet. The malfunctioning valve indicated that the larger amount of small eddy formed on the side of the valve and sinus near the fully open which is a functioning valve. More areas of turbulent flow and higher turbulence dissipation are generated due to a big amount of blood flowing through. The flow rate is directly proportional to the eddy intensity. This means that an increase in flowrate can increase the eddy intensity and distribution of hemolysis (James, Papavassiliou and O'Rear, 2019).

2.3 Vortex Generator

For eras, VGs were used in airline transport and military aircraft. VGs are used to delay the separation and turbulent airflow through a higher angle of attack. VGs are not only applied in aerospace but in the automotive field and wind turbine too. Nowadays, VGs are widely used in the different major sector in this world to enhance their performance.

2.3.1 Vortex Generator Effect on Bluff Body

An approach to monitor the flow across a vehicle is totally different from the one applied to monitor in an airplane. For ground impact, the rotation of wheels and the complex geometries lead to a fully developed unsteady and three-dimensional complex flow. VGs have a great influence on their efficiency. There are many factors that contribute a significant role in the efficiency of VGs (Aider, Beaudoin and Wesfreid, 2010). Figure 2.4 below showed that the parameters used in the experiment.

I. The angle, α between VG blade and surface.

II. The curvilinear position of VG on the surface.

III. The wavelength, λ between two neighbouring VGs.

IV. The length of the line of VGs, which depend on the number of VGs used.

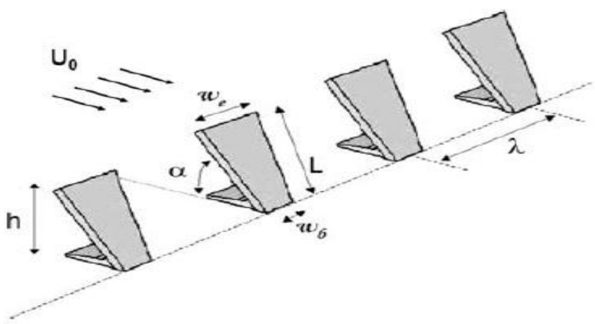

Figure 2.4: Description of VGs geometry with typical parameters used in the experiment (Aider, Beaudoin and Wesfreid, 2010).

2.3.1.1 Influence of the Angle of Vortex Generator

In the study of Aider, Beaudoin and Wesfreid (2010), it revealed that the angle of VGs is one of the parameters that influence their performance. In the simulation, 17 VGs are distributed on the bluff body surface, leading to a wavelength of 0.02m. The bluff body drag coefficient without VGs for U_o = 20m/s is C_d = 0.32 while lift coefficient, C_l = 0.46. Figure 2.5 below showed that the drag is decreased by about 12% for both cases which is α = 60° and α = 120°. The position of minimum point is the same for both cases which are s_{min} = 0.20m. In α = 60° configuration, it has a maximum lift coefficient reduction of 54%. In the conclusion, the result showed that the angle of VGs is contributed to improve the drag and lift performance in the bluff body.

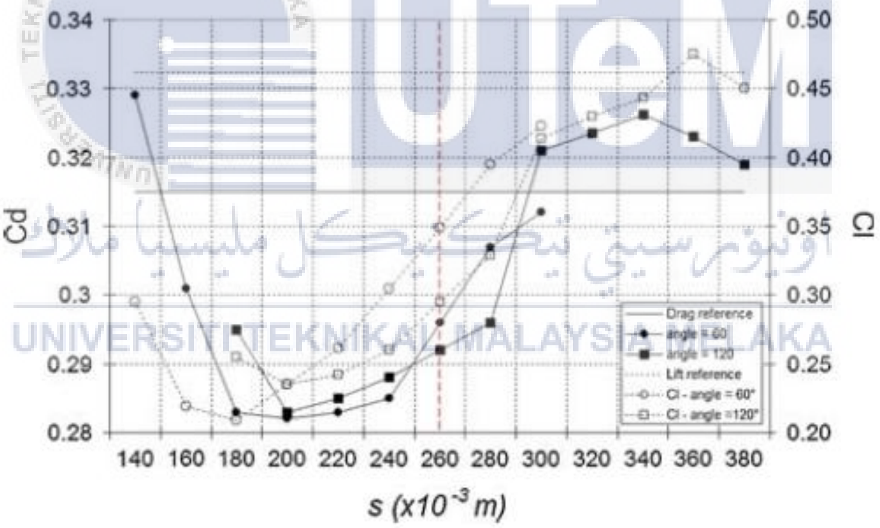

Figure 2.5: Influence of position in VGs line on drag and lift coefficients for both angles. (α=60° or α=120°) (Jean-franc and Wesfreid 2010).

2.3.1.2 Influence of the Spacing of Vortex Generator

The spacing between three-dimensional perturbation induced by VGs have a significant impact on their efficiency (Aider, Beaudoin and Wesfreid, 2010). In the research, the spacing of λ = 0.015m between VGs is used instead of λ = 0.02m. The VGs are distributed in the width of rear slant, and the number of VGs is shifted from 17 to 22. In the first observation in Figure 2.6 below, the drag and lift coefficient drop are much bigger with 0.015m spacing compared to 0.02m spacing for two different angles configuration. Next, the reduction of drag with a line of VGs is up to s = 0.32m. Figure 2.6 below concluded that the 0.015m spacing leads to a better result in both configurations.

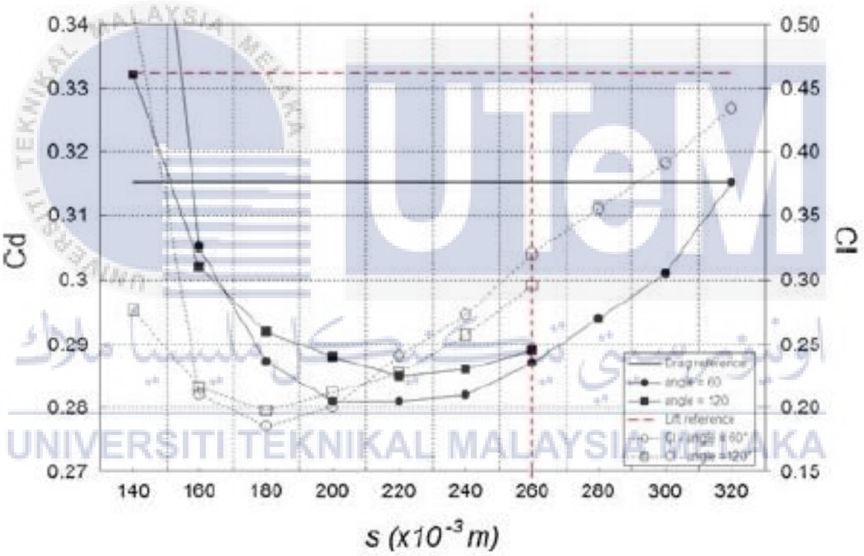

Figure 2.6: Influence of spacing between VGs with λ=0.015m instead of λ=0.02m (Aider, Beaudoin and Wesfreid, 2010).

2.3.1.3 Influence of the Reynolds Number

Different Reynolds number is investigated in this simulation. The different Reynolds number has a different value of velocity. In theoretical, higher Reynolds number with higher velocity is contributed to a turbulent flow. In Figure 2.7 below, it showed that drag reduction obtained with a given arrangement is dropping: -12.2% for U_o = 20m/s, -7.1% for U_o = 30m/s and -3.7% for U_o = 40m/s. Another study is conducted with different configuration with different angle α = 40°, U_o = 40m/s and s = 0.20m. Due to this small change, the drag reduction is increased from 3.7% to 7.1%. It validates that the impact of the angle of VGs on the surface is one of the significant parameters that influence the efficiency of VGs.

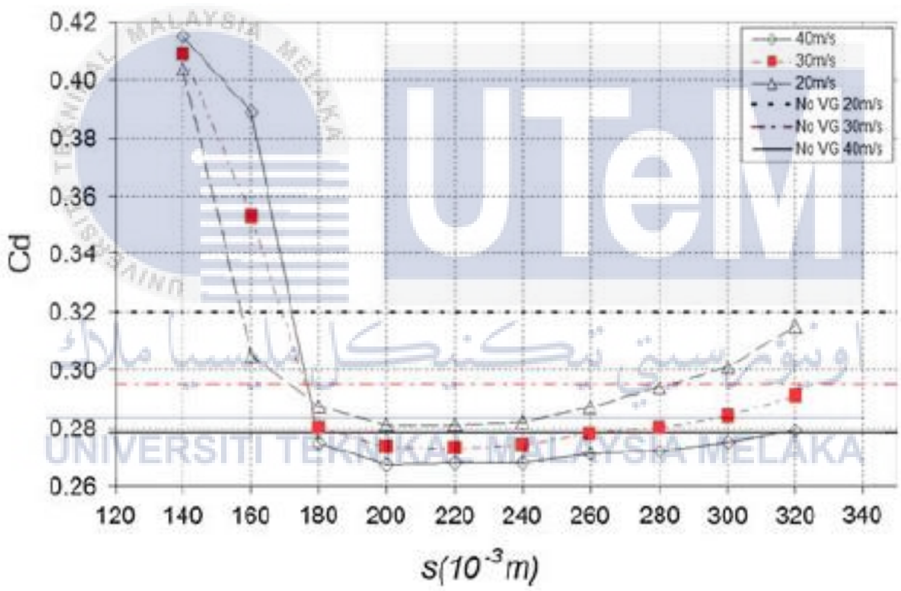

Figure 2.7: Drag reduction obtained for three different free stream velocities for Uo = 20m/s, 30m/s and 40m/s.

2.3.1.4 Influence of the distribution of vortex generators along the width of a bluff body

Figure 2.8 showed that the VGs are located at each side of the bluff body, the drag coefficient is much larger than the complete line. This result suggested that the VGs close to the side edges interact significantly with trailing vortices. On the other hand, when the VGs are located in the center of the rear slant have a more favorable effect on drag coefficient. This study concluded that the VGs in the center clearly modify recirculation bubble that leading to drag reduction. In a conclusion, eliminating VGs near to the side edges leads to a clearer drag reduction.

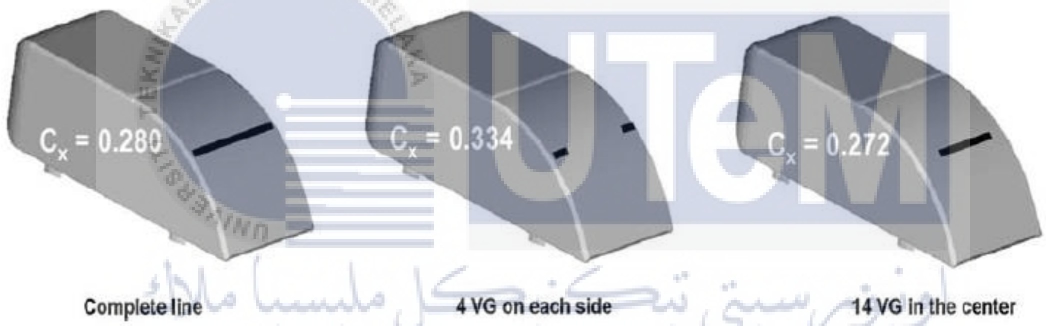

Figure 2.8: Three different arrangements of VGs along the width of the bluff body for s = 0.20m.

2.3.2 Vortex Generator Effect on Wind Turbine

VGs are widely applied to improve the performance of aerodynamic of the wind turbines and reduce the separation of flow. The VGs are oriented so it can produce longitudinal vortices to enhance high momentum fluid from the outer flow into the surface of boundary layer. According to Wang et al. (2017), the VG improved the performance of turbine airfoil and reduced the thickness of boundary layer effectively. Besides that, the double arrangement of VGs also showed a better result in controlling the separation of flow and delay emergence of the phenomenon of the stall, which is enhanced the lift coefficient of turbine airfoil and reduced the drag coefficient. The efficiency of turbine airfoil increased, which is the power output of the wind turbines is improved by 96.48%.

The thick airfoils are commonly applied to the inboard portion to improve blade strength for large-scale wind turbine blade. But airfoil appears to have poor aerodynamic efficiency due to large curvature of the upper surface and high adverse pressure gradient at the back of airfoil. Therefore, VGs are necessary to improve the aerodynamic performance of thick airfoil. VGs are effectively enhance the performance of aerodynamic. The wind turbines power output has increased by 25% due to the installation of VG in a thick airfoil blade (Zhang *et al.*, 2016).

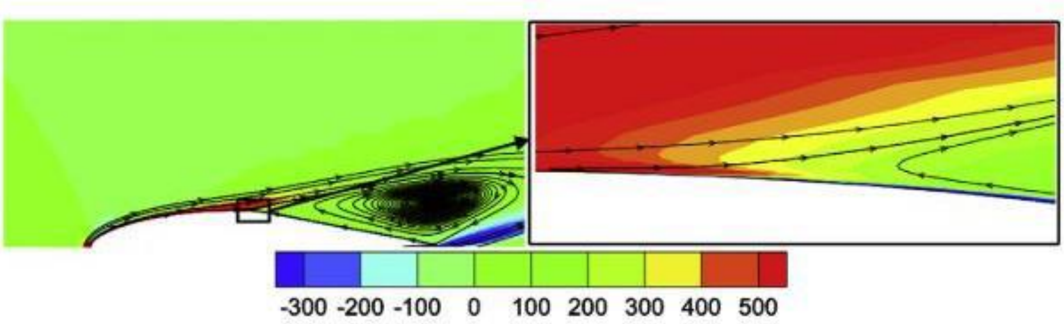

Figure 2.9: Aerodynamic Flow Pattern over Wind Turbine without VG (Wang *et al.*, 2017).

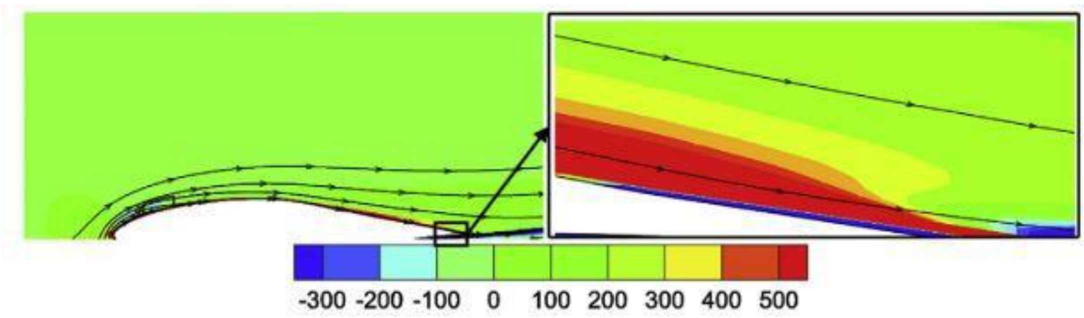

Figure 2.10: Aerodynamic Flow Pattern over Wind Turbine with VG (Wang *et al.*, 2017).

In Figure 2.9 above showed that the occurrence of flow separation on the surface of airfoil when the stall angle is 14°. The upstream fluid is removed from the boundary layer by the stagnation fluid particles. Therefore, the effect of the viscous friction and adverse pressure gradient are present, the flow separation started, and the inverse flow occurs at the airfoil's trailing edge. Due to the application of VG, there is no inverse flow occurs on the surface of the airfoil as shown in Figure 2.10 above.

2.3.3 Vortex Generator Effect on Car

Aerodynamic drag is a main concern to accelerate when it moves in the air. The drag force pulls the solid body from back to decrease the speed of the solid body and hence the fuel efficiency is affected. About 50% - 60% of total fuel energy is consumed due to aerodynamic phenomenon. The negative pressure area and the separation pressure drag can be reduced by optimizing the shape to ensure streamlining (Hassan *et al.*, 2014).

VGs are to supply momentum from large momentum at upstream flow to a smaller momentum at downstream flow by streamwise vortices generator from VGs located before the separation point. It helps to reduce the drag by delaying the separation. The appearance of VGs is conducted in the study of C and Thiyagarajan (2015). It showed that the VGs diverged the flow of air is the most effective approach to reduce the drag in car. It is followed by VGs convergent orientation and VGs straight orientation. The research also showed that the straight orientation of VGs is giving the same effect without VGs. Figure 2.11 showed that the huge differences between VGs and without VGs. Obviously, the separation is delayed by streamwise vortex in the car body with the installation of VGs.

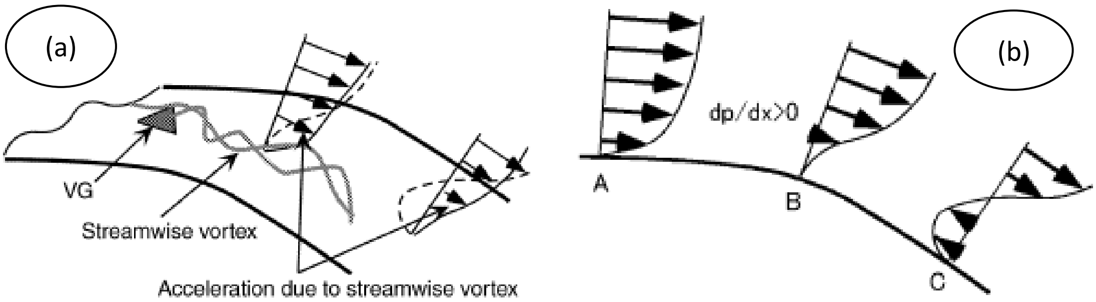

Figure 2.11: The differences of velocity profile generated between car (a) with VGs and (b) without VGs (C and Thiyagarajan, 2015).

Figure 2.12: Velocity Contour of a Body without VG (C and Thiyagarajan, 2015).

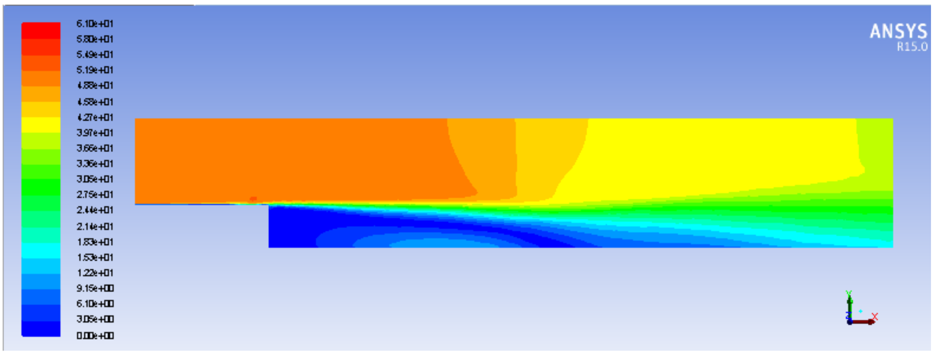

Figure 2.13: Velocity Contour of a Body with VG (C and Thiyagarajan, 2015).

Both Figure 2.12 and Figure 2.13 are showed that the huge difference in velocity contour. The body has larger drag reduction as shown in Figure 2.13 which is the body with the application of VGs. The maximum velocity can be obtained in the body without VGs which is 51.11 m/s while the maximum velocity in the body with VGs is 61m/s. It showed that the aerodynamic drag is contributed toward the body and hence reduces the velocity of the body.

2.3.4 Vortex Generator Effect on Prosthetic Heart Valve

Blood clotting is an inherent issue with the present of BMHV designs. The reduction of pressure gradients and turbulent flow are studied by controlling the orientation of VGs. In the investigation, the Co-Rotating VGs is reduced Reynolds shear stresses and improved the pressure gradient. Co-rotating VGs as shown in Figure 2.14, it induced a more delayed flow. The Co-Rotating equally spaced VGs showed that it is the most optimal case in improving the pressure gradient and minimal turbulence. VG aided to diminish the hemodynamic factors which are blood clotting for a better and more ideal mechanical valve design (Hatoum and Dasi, 2019).

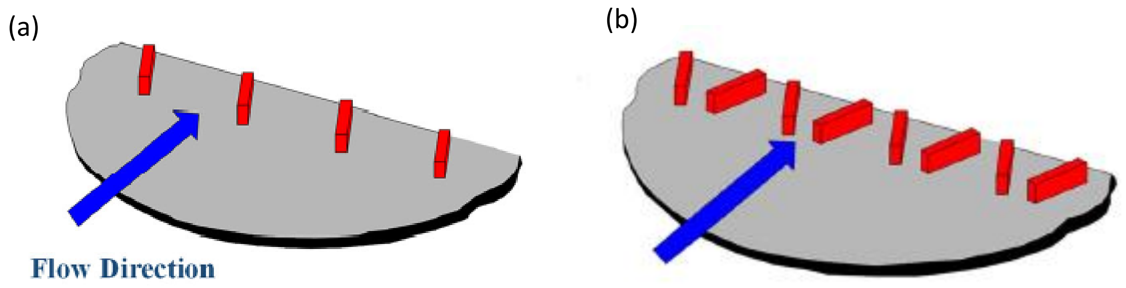

Figure 2.14: (a) Co-rotating Equally Spaced of VG and (b) Counter Rotating Closely Spaced on Bi-leaflet Mechanical Heart Valve (Hatoum and Dasi, 2019).

Table 2.1: Summary of Hemodynamic Data in Different VGs Arrangements (Hatoum and Dasi 2019).

	Control valve	Co-rotating VGs	8 counter-rotating equally spaced VGs	4 far spaced counter-rotating VGs	4 closely spaced counter-rotating VGs
Pressure gradient (mmHg)	14.88 ± 0.40	10.45 ± 0.94	13.76 ± 0.51	13.84 ± 0.09	15.37 ± 0.16
Effective orifice area (cm^2)	1.43 ± 0.04	2.26 ± 0.17	1.58 ± 0.05	1.53 ± 0.02	1.42 ± 0.01

Table 2.1 indicated that the Co-Rotating VGs has lower pressure gradient and higher Effective Orifice Area (EOA) between five different arrangement. EOA is a tool of measure of prosthetic heart valve efficiency. With the optimal arrangement of VGs, the pressure gradient has significantly reduced and hence the probability of platelet activation and thrombus formation also decreased.

2.4 CFD in Mechanical Heart Valve

Computational Fluid Dynamic (CFD) is the discipline of science devoted to predicting fluid flow by solving mathematic models that governing these processes by using numerical method. CFD simulations are relatively inexpensive and enable a designer to simulate different types of conditions. In the biomechanical field, CFD simulations are currently used models demonstrate the possibility to enhance hemodynamic properties at the position of high shear stress and boundary layer of the leaflets (Zbavitel and Fialová, 2019).

CFD simulation can model three-dimensional BHMV flow with high spatial resolution and temporal resolution in which the smallest level of fluid motions can be solved. CFD was conducted to model pulsatile BMHV flow with adults by using a validated suspension flow solver to model large BMHV flows and accurately quantify platelet damage (Yun, McElhinney, *et al.*, 2014). Studies in CFD to simulate flow through BMHV often motivate the blood damage to predicting hemolysis. CFD also can used to capture the relative extent area to trigger blood damage. The heart valve simulations results are validated and give confidence to other results obtained (James, Papavassiliou and O'Rear, 2019).

CHAPTER 3

METHODOLOGY

3.1 Introduction

This chapter explains that the entire process of project with an illustration of the flow chart as shown below. The computational fluid dynamic (CFD) software, ANSYS Workbench 16.1 is used to perform all the simulations. The CFD setup, pre-processing and post-processing are discussed in methodology. The simulation results are compared to the research of Yun, Dasi et al. (2014) for validation and verification purposes. Next, the simulation with vortex generators is generated to identify the solutions to decrease the pressure gradient and Reynolds shear stress to reduce blood clotting formation.

The overall methodology of the flow chart is shown in Figure 3.1 below. The methodology was started sketching an idealized geometry followed by the standard research of Yun, Dasi et al. (2014). Then, the simulation of laminar flow and turbulent flow were simulated in ANSYS Workbench 16.1 with Reynolds Number of 750 and 5000 respectively through an idealized geometry. The result of the simulation was compared to the experiment result of Yun, Dasi et al. (2014) for validation purposes. After the validation was completed, the vortex generator was installed on the leaflet to determine the result of simulation in terms of pressure drop between the position of after leaflet and before leaflet. If the pressure gradient was reduced, it meant that the application of vortex generator was crucial to reduce the complication of mechanical heart valve. Furthermore, the best model of orientation of VG was chosen from three designed model. Turbulent transient pulsatile flow simulation was processed in simplified geometry without VG and the best model of VG. As a result, the turbulent kinetic energy (TKE) and turbulence shear stress were determined for further study.

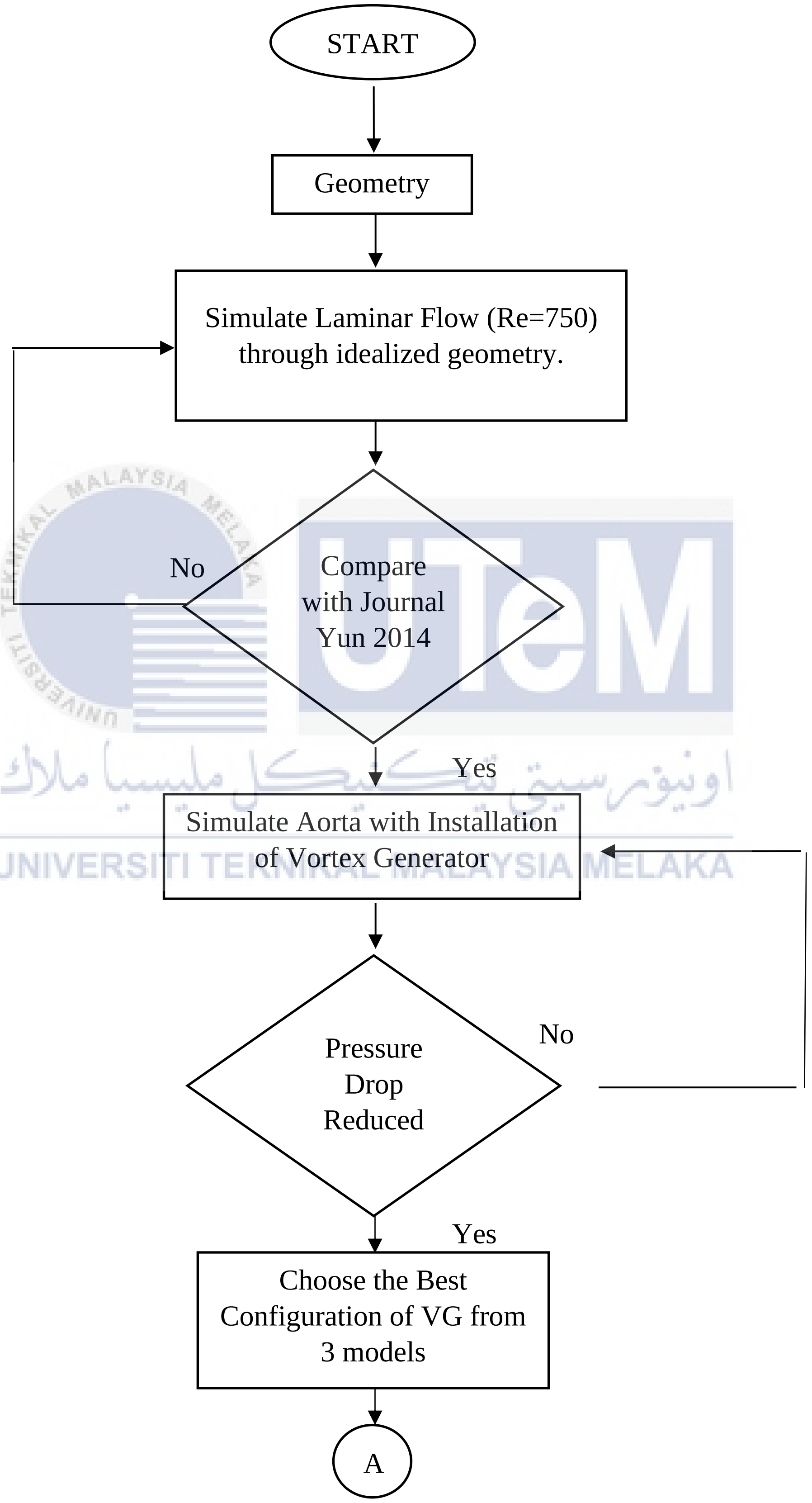

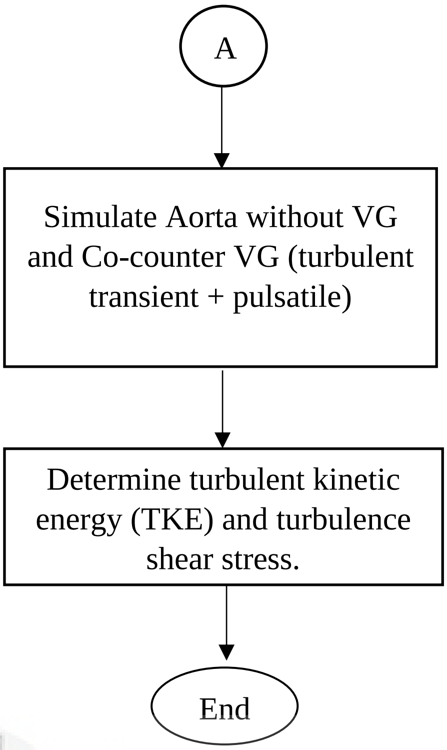

Figure 3.1: Flow Chart of the Methodology.

3.2 Idealized Prosthetic Heart Valve

The computational model was used in the simulation is shown below. This is an idealized geometry which is a flow chamber with the SJM valve according to Yun, Dasi et al. (2014). The chamber is considered a rigid straight tube with a diameter 25.4mm. The inner diameter of the valve is 21.4mm. Downstream of the valve on an aortic side is approximately expand to 31.75mm to represent the idealized aortic sinus root. The leaflets design is followed by the design of St. Jude Medical BMHV. In this research, the leaflets are considered as a fully open condition which is 5° to the horizontal. The general idea of an idealized prosthetic heart valve is shown in Figure 3.2 below.

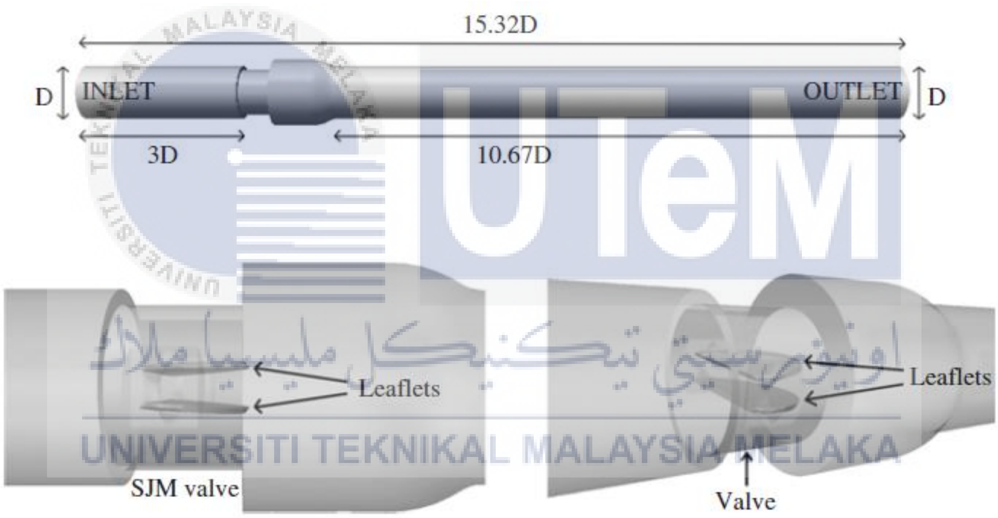

Figure 3.2: Computational Model of the Idealized Prosthetic Heart Valve (Yun, Dasi, *et al.*, 2014).

3.3 Vortex Generator

Vortex generator is designed to reduce the pressure drop in this project. The VG dimension (0.75 x 0.28 x 1) mm is shown in Figure 3.3 below, and it is a rectangular-shaped.

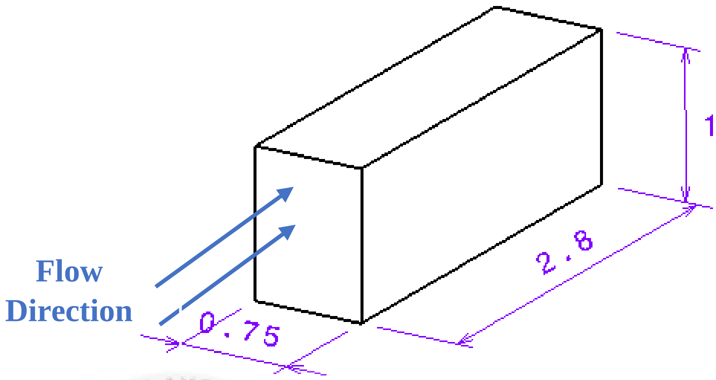

Figure 3.3: Parameters of a Rectangular Vortex Generator Design.

3.4 Boundary Condition

The boundary conditions are followed closely according to the research of Yun, Dasi et al. (2014). The blood is modelled computationally as an incompressible Newtonian fluid. The properties of human blood are defined as 1060 kg/m^3 in density. The wall is considered a rigid wall. Thus, the wall of the tube is defined as a zero-slip wall which is the fluid that has zero velocity relative to the boundary. The velocity inlet of the human blood is calculated by Eq. (1). A stress-free boundary condition is applied at outlet of the domain.

$$Re = \frac{\rho \frac{2}{3} V D}{\mu} = \frac{\frac{2}{3} V D}{\nu} \tag{1}$$

Where Re is the Reynolds Number, ρ is the density of fluid flow in kg/m^3, V is the mean velocity in the pipe in m/s, D is the diameter of the tube in meter, μ is the dynamic viscosity in kg/ms and ν is the kinematic viscosity in m^2/s.

Table 3.1: Simulation Parameters of Steady Flow-through Idealized Geometry.

Boundary Conditions	Laminar Steady Flow (Re = 750)	Turbulent Pulsatile Flow (Re = 5000)
Density of Fluid Flow (kg/m^3)	1060	1060
Dynamic Viscosity (kg/ms)	5.9831×10^{-3}	2.5556×10^{-3}
Kinematic Viscosity (m^2/s)	5.6444×10^{-6}	2.4110×10^{-6}
Diameter of Tube (m)	0.0254	0.0254
Inlet Velocity (m/s)	0.25	-0.3726 ~ 0.7119
Outlet Pressure (Pa)	0	0

A dimensionless number of pulsatile flow frequency (Womersley number) in a relation to viscosity is calculated by using Eq. (2). For the pulsatile of BMHV flow, the Womersley number (W_n = 1~1.3) is used in current project. The pulsatile flow in BMHV consists of four stages which are acceleration stage, peak stage, deceleration stage and diastole stage.

$$W_n = \frac{D}{2}\sqrt{\frac{\omega}{\nu}} \tag{2}$$

Where ω is the angular velocity of pulsatile flow, D is the inlet diameter and ν is the kinematic viscosity.

The inlet of the flow in the CFD simulation required the application of the User-Defined Function (UDF). The parabolic velocity profile was written in C programming language as shown in Figure 3.4 below. The parabolic program file was built and loaded in ANSYS FLUENT component system through the User-Defined Function “interpret” feature. In the other hand, pulsatile velocity profile also was written in C programming language as shown in Figure 3.5 below. The graph is illustrated in Figure 3.6 below (Raser *et al.*, 2008).

```
#include"udf.h"
DEFINE_PROFILE(velocity, thread, position)
{
/* This UDF applies a parabolic velocity profile to the boundary surface hooked in Fluent */
/* This operates for 3D models in any orientation */
/****************************/
/* THE USER INPUTS */
/****************************/
/* the centroid of the boundary face (x0,y0,z0) */
real x0 = 0.000000;
real y0 = 0.000000;
real z0 = 0.090310;
/* the maximum radius of the pipe and maximum centerline veloicty of the parabola */
real Max_Radius = 0.0127; /* diameter of the pipe Max_Radius */
real Peak_Velocity = 0.25; /* maximum centerline velocity of the parabola */
/****************************/
/****************************/

/****************************/
/* Main Program */
/****************************/


begin_f_loop(f,thread)
{
F_CENTROID(x, f, thread); /* the coordinates of the current face/element centroid accessed by F_CENTROID */

/* Radius from central axis of parabola is */
if (ND_ND==2) /* for 2D modelling */
{
r = pow(pow((x[0]-x0),2)+pow((x[1]-y0),2),0.5);
}
if (ND_ND==3) /* for 3D modelling */
{
r = pow(pow((x[0]-x0),2)+pow((x[1]-y0),2)+pow((x[2]-z0),2),0.5);
}
/* Write Profile in x */
Velocity_Profile = Peak_Velocity*(1.0-((r*r)/(Max_Radius*Max_Radius)));

/* Write velocity boundary condition */
F_PROFILE(f, thread, position) = Velocity_Profile; /* Apply velocity profile to selected boundary */
}
end_f_loop(f, thread)
/****************************/
/****************************/
}
```

Figure 3.4: Parabolic Velocity Profile in UDF C Programming Code.

```c
#include "udf.h"//file that contains definitions for define functions and fluent operations

#define PI 3.141592654

DEFINE_PROFILE(inlet_velocity,th,i)
{
        float x[ND_ND]; /* an array for the coordinates */
        float xx, y, r;
        face_t f;
        r = 0.0127; /* inlet radius in m */
        begin_f_loop(f,th)

                double t = (CURRENT_TIME*1.075269-floor(CURRENT_TIME*1.075269))/1.075269; //t is the local time within each period
                double k1, k2, k3, k4, k5, k6, k7, k8;
                double A1 = 0.45;       double m1 = 0.14;       double s1 = 0.12;
                double A2 = -0.13443;   double m2 = 0.4;        double s2 = 0.06;
                double A3 = 0.04;       double m3 = 0.65;       double s3 = 0.12;
                double A4 = 0.2;        double m4 = 0.1;        double s4 = 0.038;
                double A5 = -0.04;      double m5 = 0.37;       double s5 = 0.024;
                double A6 = -0.085;     double m6 = 0.53;       double s6 = 0.082;
                double A7 = -0.355;     double m7 = 0.058;      double s7 = 0.066;
                double A8 = -0.01;      double m8 = 0.93;       double s8 = 0.08;
                F_CENTROID(x,f,th);
                xx = 0; /* x coordinate */
                y = 0;   /* y coordinate */
        {

                k1 = A1*exp(-1*((pow(t-m1,2)/(2*pow(s1,2)))));
                k2 = A2*exp(-1*((pow(t-m2,2)/(2*pow(s2,2)))));
                k3 = A3*exp(-1*((pow(t-m3,2)/(2*pow(s3,2)))));
                k4 = A4*exp(-1*((pow(t-m4,2)/(2*pow(s4,2)))));
                k5 = A5*exp(-1*((pow(t-m5,2)/(2*pow(s5,2)))));
                k6 = A6*exp(-1*((pow(t-m6,2)/(2*pow(s6,2)))));
                k7 = A7*exp(-1*((pow(t-m7,2)/(2*pow(s7,2)))));
                k8 = A8*exp(-1*((pow(t-m8,2)/(2*pow(s8,2)))));

                F_PROFILE(f,th,i) = (1/0.39)*(k1 + k2 + k3 + k4 + k5 + k6 + k7 + k8)*(1.-(xx*xx+y*y)/(r*r));
        }
        end_f_loop(f,th);
}
```

Figure 3.5: Pulsatile Velocity Profile in UDF C Programming Code.

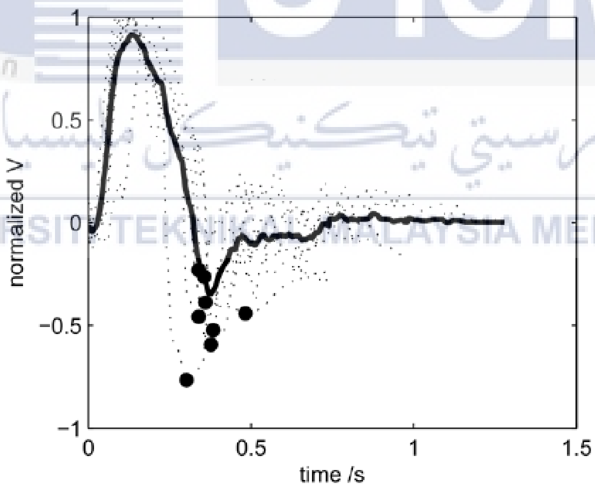

Figure 3.6: Pulsatile Velocity Profile.

3.5 Governing Equation

There are some of the equations are solved in Computational Fluid Mechanic (CFD) software. The equations are continuity equation and momentum equation. Both equations are under Navier-Stokes Equations. Besides that, the selection k-ε turbulence model is discussed in this section.

3.5.1 Navier-Stokes Equation

Blood flow is governed by using incompressible Navier-Stokes Equation. The general equations of incompressible Navier-Stokes Equation are shown below.

Continuity equation:

$$\frac{\delta\rho}{\delta t} + \nabla . (\rho \mathrm{v}) = 0 \tag{3}$$

Considered incompressible is equivalent to constant density fluid.

$$\nabla . (\rho \mathrm{v}) = 0 \tag{4}$$

$$\frac{\delta(\rho u)}{\delta x} + \frac{\delta(\rho v)}{\delta y} + \frac{\delta(\rho w)}{\delta z} = 0 \tag{5}$$

Where t is the time, ρ is the fluid density in kg/m^3 and v is the flow velocity vector field in m/s.

Momentum equation:

$$\rho\left(u\frac{\delta u}{\delta x} + u\frac{\delta u}{\delta y} + u\frac{\delta u}{\delta z}\right) = -\frac{\delta P}{\delta x} + \mu(\frac{\delta^2 u}{\delta x^2} + \frac{\delta^2 u}{\delta y^2} + \frac{\delta^2 u}{\delta z^2}) \tag{6}$$

$$\rho\left(u\frac{\delta v}{\delta x} + u\frac{\delta v}{\delta y} + u\frac{\delta v}{\delta z}\right) = -\frac{\delta P}{\delta x} + \mu(\frac{\delta^2 v}{\delta x^2} + \frac{\delta^2 v}{\delta y^2} + \frac{\delta^2 v}{\delta z^2}) \tag{7}$$

$$\rho\left(u\frac{\delta w}{\delta x}+u\frac{\delta w}{\delta y}+u\frac{\delta w}{\delta z}\right)= -\frac{\delta P}{\delta x}+\mu(\frac{\delta^2 w}{\delta x^2}+\frac{\delta^2 w}{\delta y^2}+\frac{\delta^2 w}{\delta z^2})$$

(8)

Where ρ is the fluid density in kg/m^3, P is the pressure in Pa and u, v, w is the velocity in x, y, z direction with unit m/s.

As discussed above, the first term on the RHS in equations above refers to pressure forces, $\nabla \cdot P$. The RHS describes viscous forces, $\mu\nabla^2 v$. The LHS is the change of momentum that any element experiences as it moves between regions of different velocity in the flow field. This has the dimensions of a force and is referred to as the inertia force, $\rho v \cdot \nabla v$.

3.5.2 Turbulence Model

In this study in turbulent flow, the two-order accuracy of the k-ε equation is applied in the simulation. The k-ε equation is applicable for free-shear flow and suitable for transition turbulent. On the other hand, it also suitable for low-Re internal flows which are Re is less than 10000. The k represented as turbulent kinetic energy and ε represented turbulent dissipation rate. The turbulent kinetic energy and turbulent dissipation rate are calculated by using Eq. (9) and Eq. (11) below.

$$k = \frac{3}{2}\,(UI)^2 \tag{9}$$

$$I = 0.16\,{Re_{d_h}}^{-\frac{1}{8}} \tag{10}$$

$$\varepsilon = {C_\mu}^{\frac{3}{4}}\,\frac{k^{\frac{3}{2}}}{l} \tag{11}$$

Where U is the mean flow velocity, I is the turbulence intensity which is calculated by using Eq. (10), C_μ is the turbulence model contact (0.09) and l is the turbulent length scale.

3.6 Vortex Generator Configuration

There are several types of configurations are used to test in this study. The details of the VG configuration are shown in Table 3.2 below. The angle incidence of the flow direction is about 23° based on Hatoum and Dasi (2019). The geometry of the VG will be substituted by using the design of VG shown in Figure 3.3.

Table 3.2: Details of Vortex Generator Arrangement Used in this Study.

Types of VG Configuration	**Descriptions**
Co-rotating Equally Spaced 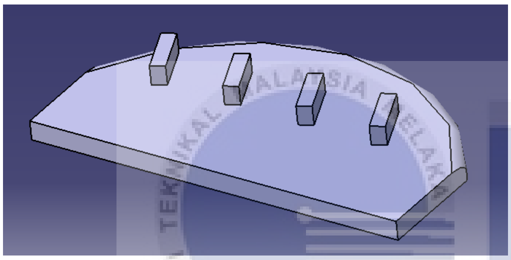	- Angle of incidence of 23°. - 4mm spacing between VG. - 5mm distance between beginning of leaflet and VG. 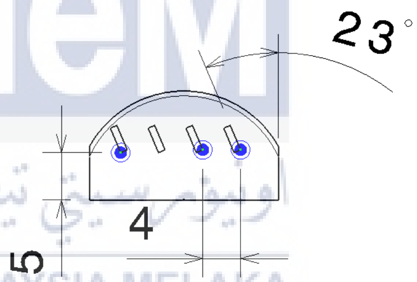
Straight Equally Spaced 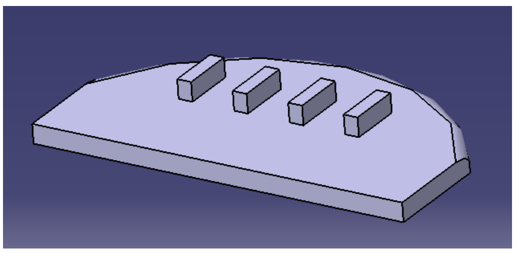	- 3mm spacing between VG. - 5mm distance between beginning of leaflet and VG. 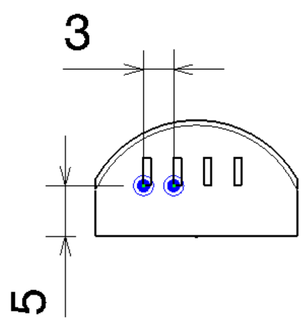

Counter-rotating Far Spaced 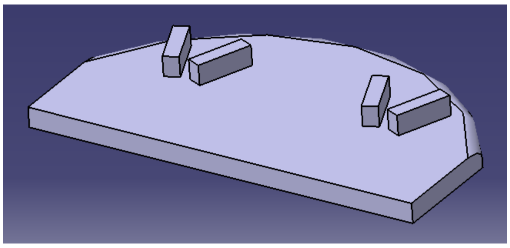	- Angle of incidence of 23°. - 8.5mm distance in middle gap. - 0.5mm distance between two VG. - 5mm distance between beginning of leaflet and VG. 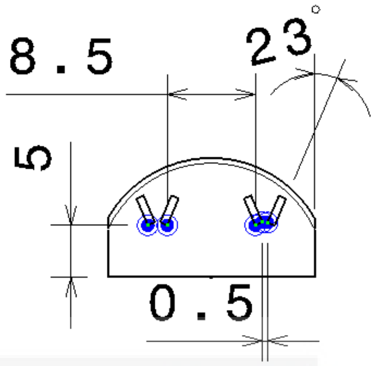

3.7 Turbulence Shear Stress

Turbulence and platelet activation are correlated to turbulence shear stress. It also known as Reynolds Shear Stress (RSS). Turbulence shear stress is recorded at the crucial area where leaflets are located. The turbulence shear stress was computed using Eq. (12).

$$Turbulence\ Shear\ Stress = \mu\frac{du}{dz} + \eta\frac{d\bar{u}}{dz} \tag{12}$$

Where μ is the dynamic viscosity in kg/ms, u is the velocity in m/s, z is the distance from inlet in m, η is the eddy viscosity in kg/ms and $\bar{u}$ is the average velocity magnitude in x-y-z direction in m/s.

3.8 CFD Simulation Setup

There are few main steps in CFD simulation. The steps are categorised to pre-processing, solver and post-processing. The setup details of pre-processing and solver are discussed in section below.

3.8.1 Boundary Named Selection

The idealized geometry was labelled by creating a boundary named selection as shown in Figure 3.7.

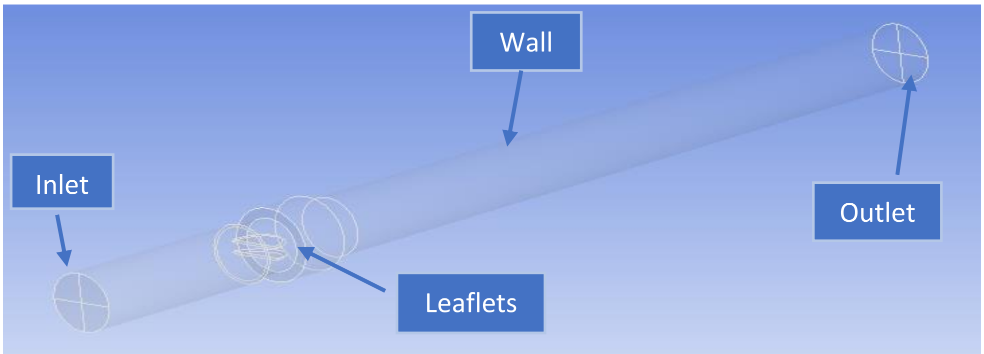

Figure 3.7: Boundary Named Selection in Idealized Geometry.

3.8.2 Meshing

There are three regions with boundary named selection required a finer meshing to get a better data result. These leaflet regions were the focus to capture the velocity profile in the idealized geometry.

For the wall boundary, the inflation was applied with the first layer height of 1 mm, maximum layer of 5 and growth rate of 1.1. The entire geometry was applied with body sizing with the body of influence method to enhance the elements around the leaflets and central flow as shown in Figure 3.9. The meshing elements around the two leaflets were finer after the body sizing method. The number of meshing elements without the vortex generator is shown in Table 3.3 below. Figure 3.8 showed that the view of the geometry with the meshing grid.

Table 3.3: Statistics of meshing grid.

Statistics	**Numbers / Values**
Nodes	353580
Element	1558894
Orthogonal Quality (Min)	0.24615
Skewness (Max)	0.79563

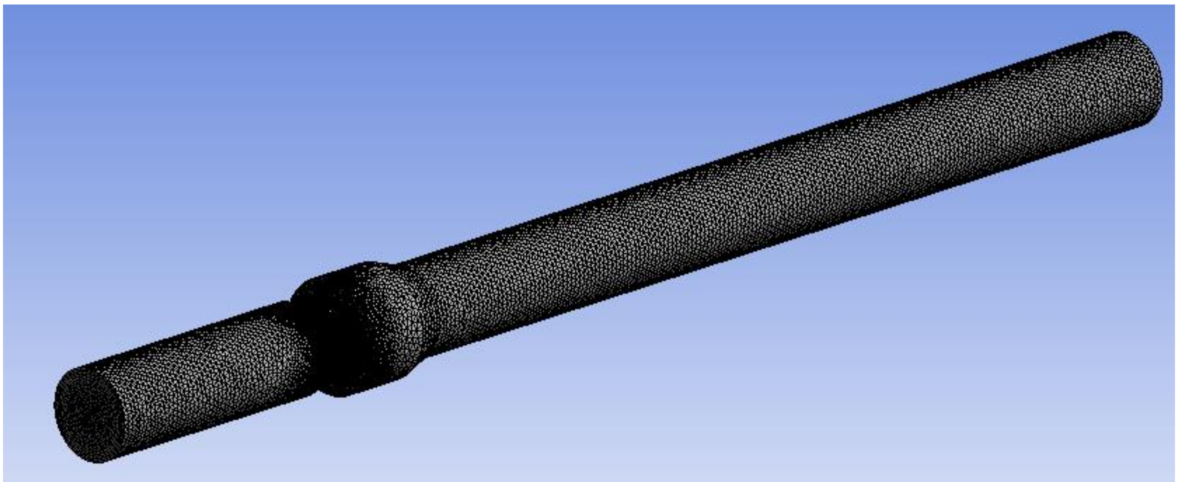

Figure 3.8: Tetrahedral meshing grid.

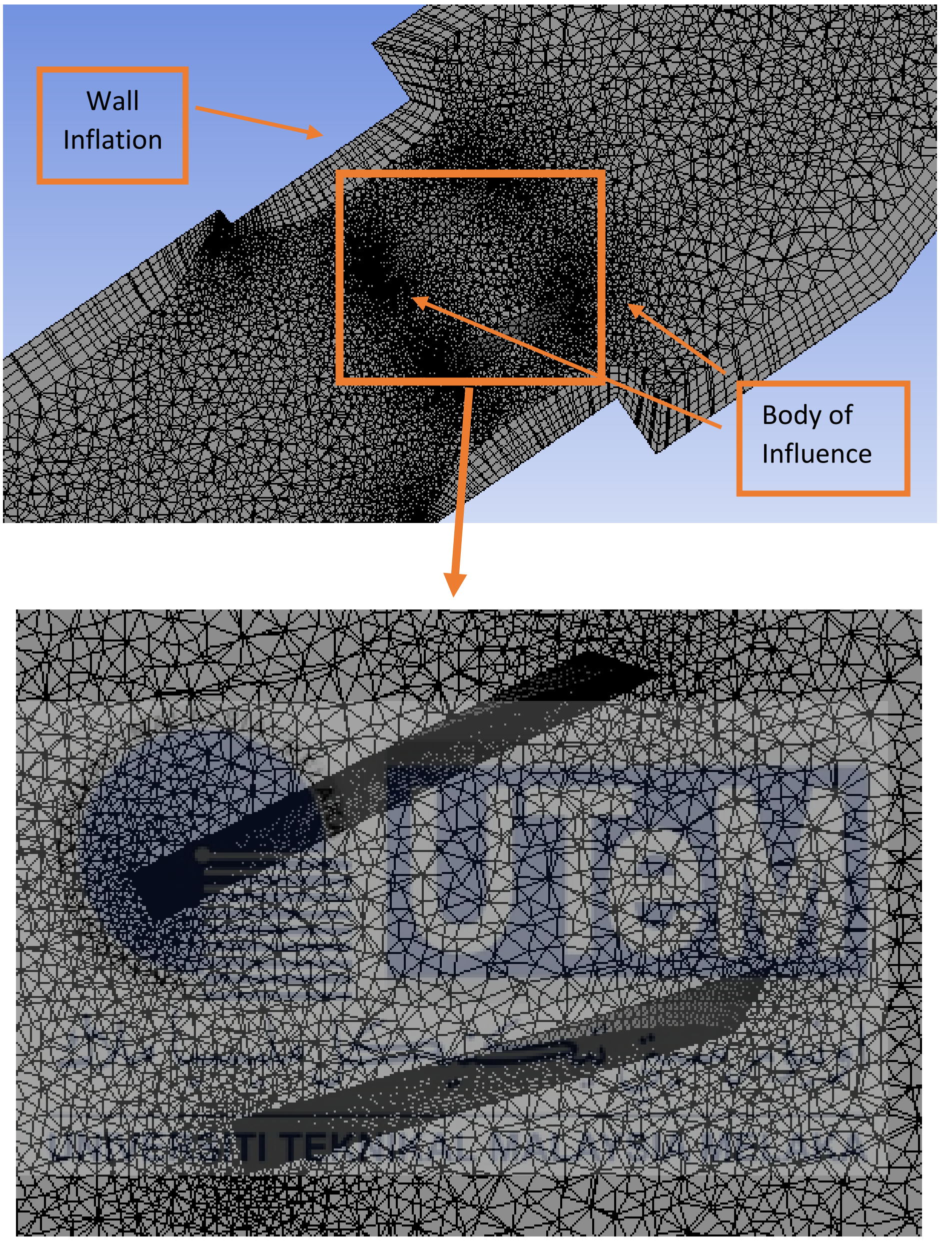

Figure 3.9: Topology of the grid.

3.8.3 Solver

The Coupled Algorithm was applied for Pressure-Velocity Coupling while Gradient is the Least Square Cell-Based. The solution of discretization of components are shown in **Table 3.4** below. The monitor of residuals was set as absolute convergence criterion. The convergence criteria were set in 0.001.

Table 3.4: The Solution of Discretization.

Components	Method
Pressure	Second Order
Continuity	Second Order Upwind
Momentum	Second Order Upwind
Turbulent Kinetic Energy	Second Order Upwind
Turbulent Dissipation Rate	Second Order Upwind

3.9 Grid Independent Test

In Grid Independent Test, there are three different type of meshing is applied in the comparison to study the sensitivity: Coarse, Medium and Fine. The grid quality is determined by using 0.1 of ratio in number of gaps across cell and transition ratio in inflation. The pressure should approach the same answer when the grid size is become finer. Table 3.5 below showed the details of each mesh quality settings. In Figure 3.10 showed that the pressure against three different grid element which consider as three different of grid quality. The graph is illustrated a typically plateau type.

Table 3.5: Grid Independent Test

Grid Quality	Coarse	Medium	Fine
Elements	771482	1142991	1558894
Nodes	191603	267581	353580
Pressure (Pa)	31.97	12.51	10.07
Mass Flow Rate (kg/s)	0.067	0.067	0.067

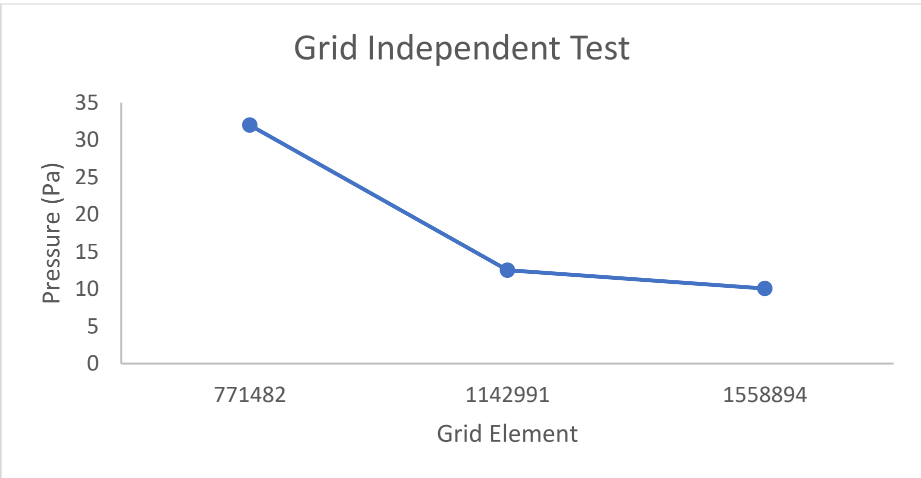

Figure 3.10: The Graph of Grid Independent Test – Pressure against Grid Element.

3.10 Validation

The velocity profile after going through the leaflets is required to be validated against Yun, Dasi et al (2014) prosthetic heart valves LBM numerical simulation result. The validation is completed by comparing the blood velocity profiles at the end tips of leaflets. The comparisons are taken in three different positions which are taken at the downstream of the end tips of leaflets: $x = 2.2mm$, $x = 10.3mm$, and $x = 20.1mm$ as shown in Figure 3.11.

In Figure 3.12, Figure 3.13 and Figure 3.14 below showed that the previous result in Yun, Dasi et al (2014) which is the maximum velocity is 0.27 m/s. The maximum velocity of the present study of simulation is followed the same as the reference. From the validation result, the velocities at the lateral orifice jet have 0.03 m/s and 0.06 m/s differences from the result of Yun, Dasi et al (2014) respectively. This is because the parameters of the geometry and the fluent setup might have some tolerances between the previous study and current study.

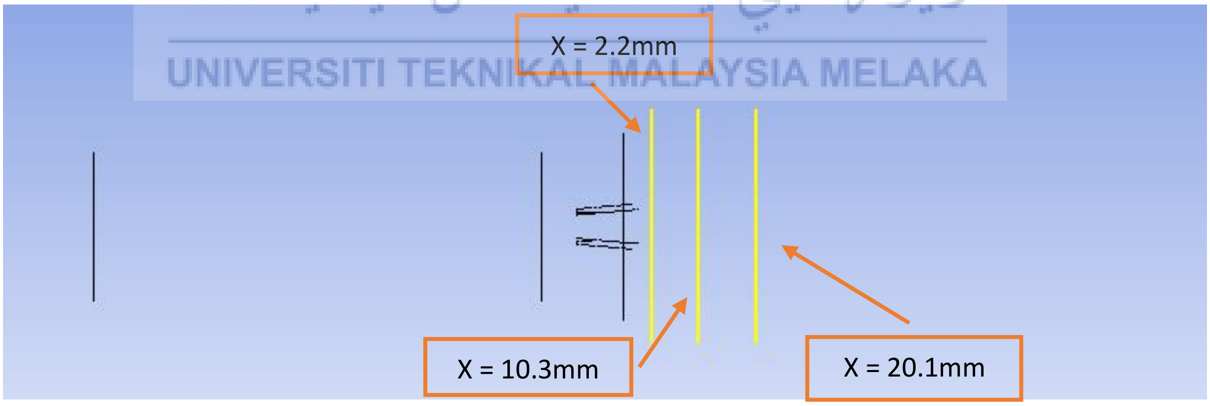

Figure 3.11: Illustration of validation location.

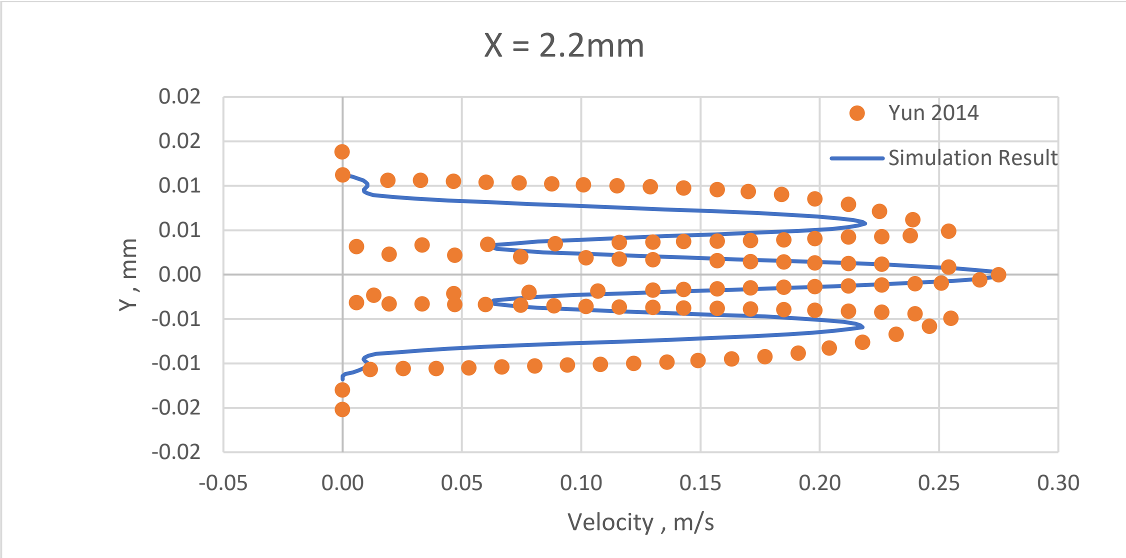

Figure 3.12: The Velocity Profile Comparison Result at x = 2.2mm.

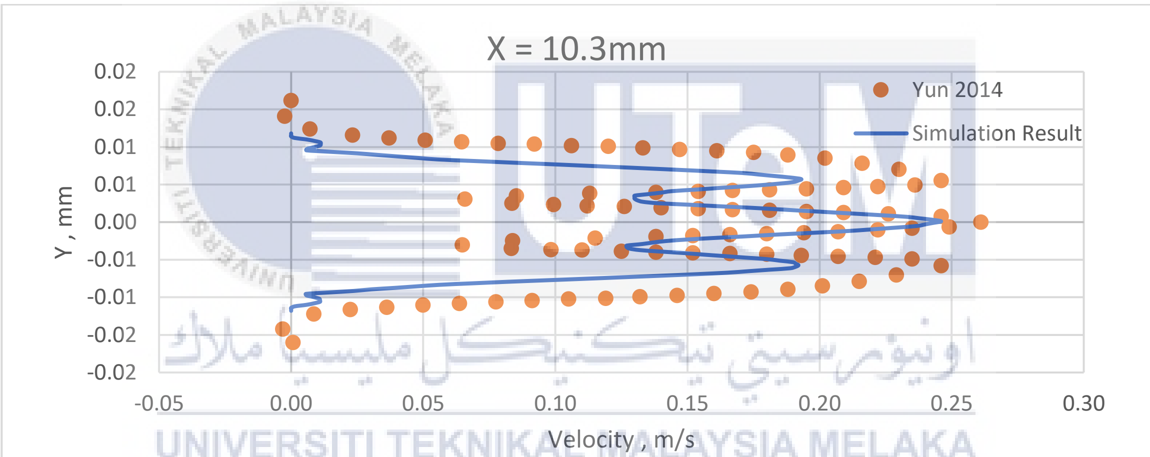

Figure 3.13: The Velocity Profile Comparison Result at x = 10.3mm.

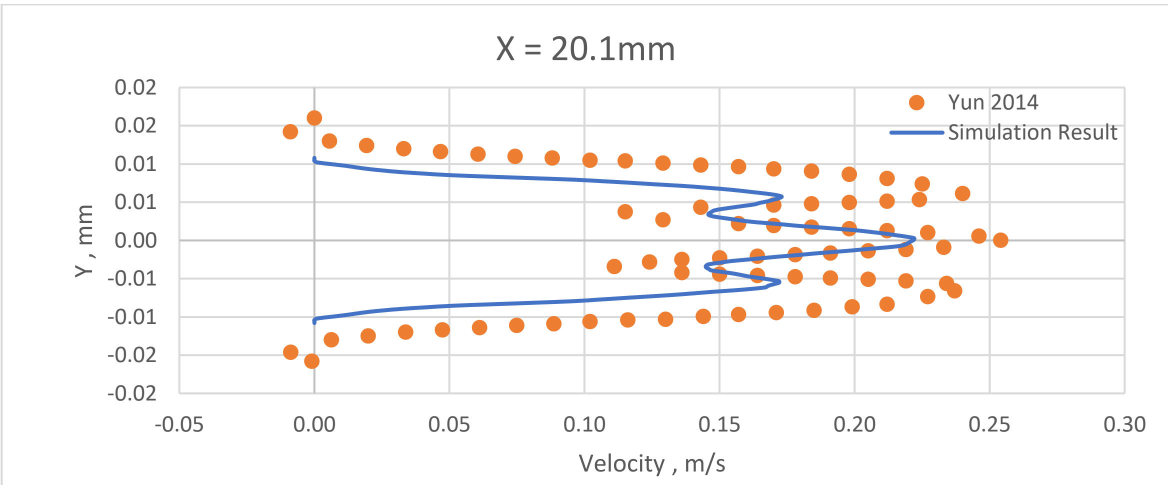

Figure 3.14: The Velocity Profile Comparison Result at x = 20.1mm.

CHAPTER 4

RESULTS AND DISCUSSION

4.1 Pressure Drop

The pressure drop exemplifies as the transvalvular pressure drop which is the key significant of hemodynamic parameter. This is because of the resistance of valve orifice area against the bloodstream when blood flows through the valve (Salleh *et al.*, 2020). Thus, there are several positions to measure the pressure drop where after leaflet and before leaflet as shown in Figure 4.1(a) below. The final positions are identified as shown in Table 4.1(b) due to the highest percentage of improvement after the several positions are compared. The simulation result of different type of VG configuration are shown in Table 4.1 below.

Figure 4.1: (a) The several points across leaflets. (b) The points chosen for comparison.

Table 4.1: Simulation Result in Pressure Drop.

Type of VG Configuration	Pressure Drop (Pa)	Percentage of Improvement (%)
Without VG	5.903	-
Co-counter Equally Spaced	3.387	42.62
Straight Equally Spaced	5.701	3.42
Counter-rotating Far Spaced	3.779	35.98

Table 4.1 above summarised that the simulation of pressure-drop in different type of VG configuration. According to Hoyoon Lee et al (2016), the pathological shear stress to activate platelets and to induce the formation of thrombus is 8 Pa. Thus, it is necessary to reduce the probability of occurrence of platelets activation in BMHV. Co-rotating Equally Spaced VG yielded the lowest pressure drop of 3.387Pa compared to others. While the Straight Equally Spaced VG and Counter-rotating Far Spaced VG yielded 5.701 Pa and 3.379 Pa respectively. The leaflets without the installation of VG generated 5.903 Pa of pressure drop.

The percentage of pressure drop difference between VG and without VG was calculated. The Co-counter Equally Spaced VG yielded the highest percentage improvement of 42.62%. The percentage improvement of Straight Equally Spaced VG and Counter-rotating Far Spaced VG were 3.42% and 35.98% respectively. It indicated that the pressure is significantly decrease after installation of VG. The results indicated that the VG was reduced separation of the boundary layer and significantly improved pressure in downstream flow in term of reducing the occurrence of hemolysis in BMHV. On the other hand, possibility of platelets activation and formation of thrombus will also diminish due to the pressure decreased.

The Co-rotating Equally Spaced VG showed the best design in reduction of pressure drop compared to Straight Equally Spaced VG and Counter-rotating Far Spaced VG. Co-counter Equally Spaced VG and Counter-rotating Far Spaced VG were depended on the type of flow separation in previous study. Nevertheless, the turbulent pulsatile flow needs to be investigated in Co-counter Equally Spaced VG and leaflets without VG.

In the aspect of VG configuration, the performance of Straight Equally Spaced VG is much poorer compared to other two models which are Co-counter Equally Spaced VG and Counter-rotating Far Spaced VG. The angle of incidence of 23° in VG orientation against the flow is very crucial. It is leaded to a better pressure reduction in prosthetic heart valve. Thus, the angle of incidence in VG configuration is one of the significant requirements to improve the complication in bi-leaflet prosthetic heart valve which is blood clotting.

4.2 Turbulence Kinetic Energy and Turbulence Shear Stress

In this simulation, prosthetic heart valve without VG and the most optimal arrangement of VG in the previous work are investigated and evaluated. Turbulence is produced by excessive kinetic energy in parts of a fluid flow. The six lines are compared and figured out the highest TKE among the lines. The line has the highest TKE is identified and the line as a reference line for turbulent shear stress calculation. The six lines are located at the leaflets where the crucial parts in this project as shown in Figure 4.2 below.

Figure 4.2: Six lines located at leaflets for comparison purpose.

Turbulent flow is categorised by chaotic change in pressure and velocity. Turbulence kinetic energy (TKE) is the mean of kinetic energy per unit mass associated with eddies in turbulent flow. The higher the kinetic energy, the more turbulence is generated. VG is a device that design to delay flow separation in turbulent flow. In Table 4.2 below, it showed that the TKE and turbulence shear stress are significantly reduced in case with VG compared to the case without VG. In simplified prosthetic heart valve with case with VG, the value of TKE is decreased about 7.82% compared to case without VG. While turbulence shear stress is reduced about 52.96% compared to case without VG.

Table 4.2: Simulation turbulence kinetic energy and turbulence shear stress result.

Type of VG Configuration	Turbulence Kinetic Energy (J/kg)	Turbulence Shear Stress (Pa)
Without VG	2.558×10^{-3}	2.487×10^{-2}
Co-counter Equally Spaced	2.358×10^{-3}	1.170×10^{-2}

Excessive kinetic energy in prosthetic heart valve without VG installation is activated higher probability of blood clotting occurrence. The higher TKE is contributed to higher turbulence. Hence, the pressure is increased in the prosthetic heart valve that lead to occurrence of blood clotting to form a thrombus. From the values of TKE and turbulence shear stress in Table 4.2, VG is played a significant role to improve the performance of prosthetic heart valve. It delayed the flow separation and reduced pressure in prosthetic heart valve. The probability of platelet activation is reduced due to the pressure decreased in prosthetic heart valve.

4.3 Contours and Streamline

In the comparison of velocity contour between case with VG and without VG, it is showed that the velocity in case VG is significantly reduced about 3.03%. In Figure 4.3, the highest velocity is 3.040x10^{-1} m/s while the highest velocity in Figure 4.4 is 2.948x10^{-1} m/s. Blood clotting may occur in the leaflets when higher velocity is generated. Thus, VG is essential to install on leaflets to reduce the blood velocity. In the velocity reduction, VG is a good device to reduce the possibility of thrombus formation. Without the installation of VG, there is abnormal flow at the vicinity of leaflets. Therefore, VG is to avoid the abnormal flow by creating small vortices at the vicinity of leaflets. The vortices are maintained the circulation and the streamwise is deteriorate slower compared to the case without VG.

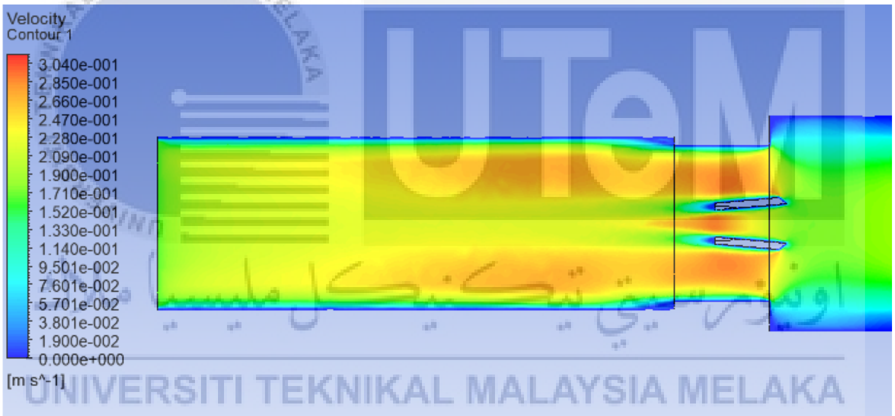

Figure 4.3: Velocity contour in non-VG case.

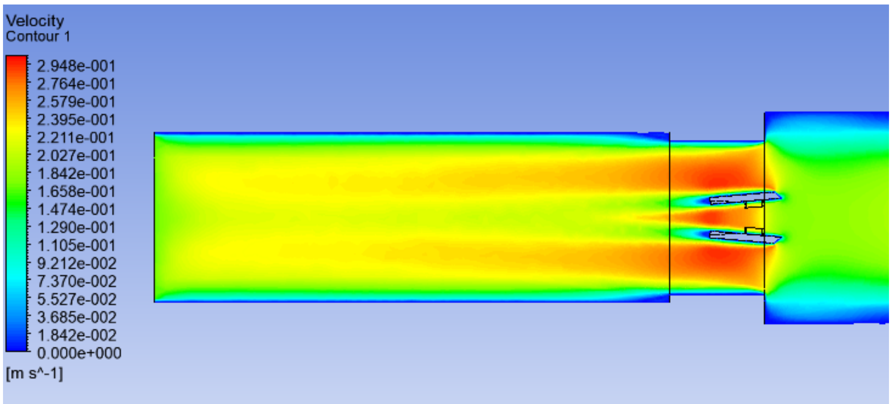

Figure 4.4: Velocity contour in VG case.

In comparison of turbulence kinetic energy between case VG and without VG, it showed that the turbulence kinetic energy is reduced about 5.5%. The average TKE in non-VG case is 1.182 J/kg while the average TKE in VG case is 1.117 J/kg. The average TKE is determined by using a plane where located at x = 0.00m in yz-plane along the prosthetic heart valve. The higher the value of TKE is generated, the higher possibility of thrombus formation. Therefore, VG is installed to control the flow and reduce the possibility of blood clotting. In Figure 4.6 below, VG is effectively to mitigate the TKE by delaying the flow separation compared to non-VG case shown in Figure 4.5 below.

Figure 4.5: Turbulence kinetic energy contour in non-VG case.

Figure 4.6: Turbulence kinetic energy contour in VG case.

In streamline pattern showed that the flow separation is delayed in Figure 4.7 below. The wake region is located after the leaflets. The flow separation is delayed after the installation of VG on the leaflets as shown in Figure 4.8 below. It showed that the crucial properties are reduced due to the installation of VG on the leaflets. For example, the turbulence shear stress, turbulence kinetic energy and velocity are decreased as explained in previous discussion. Figure 4.8 showed that the velocity at the central jet is more streamwise compared to the case without VG. Vorticity in the shear layer dissipate faster in the case without VG. This phenomena in leaded to no circulation at the vicinity of leaflets due to fastest decay in streamwise. In these simulation results, it clearly indicated that the VG is very crucial device to enhance the performance of mechanical prosthetic heart valve in current market. It can significantly reduce the pressure across the leaflets and reduce the probability of hemolysis which is the formation of thrombus.

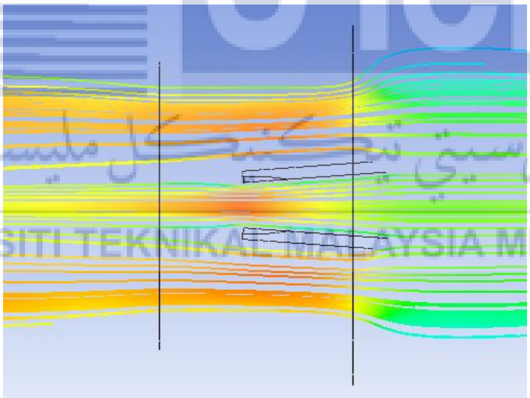

Figure 4.7: Streamlines pattern across leaflets in non-VG case.

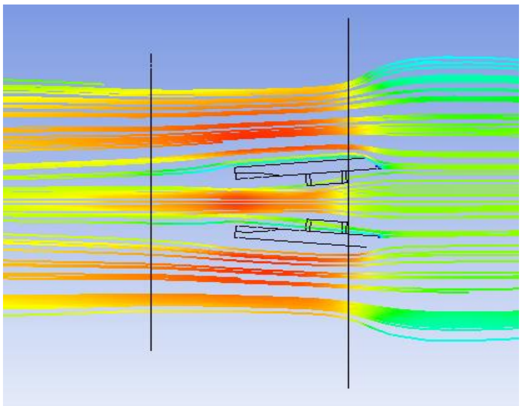

Figure 4.8: Streamlines pattern across leaflets in VG case.

4.4 Comparison in Different Phase of Pulsatile

To better envision the variation of velocity for each phase in pulsatile, Figure 4.10, Figure 4.11 and Figure 4.12 are showed the velocity profile longitudinal direction against Y (mm) along the prosthetic heart valve at the position right after the leaflets as shown in Figure 4.9 below. The position of line is at X = -0.004m from origin.

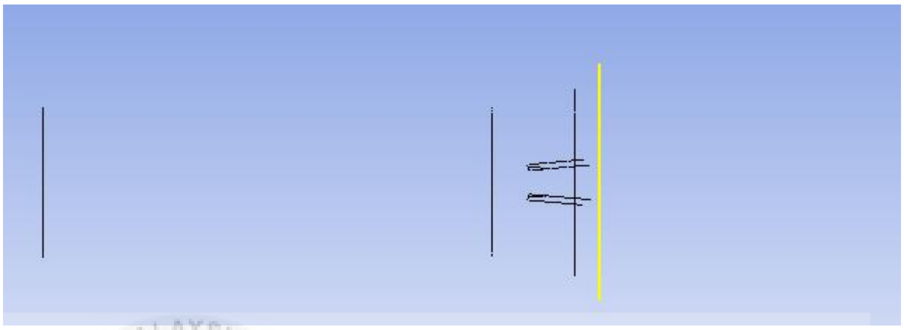

Figure 4.9: The position of line at X = -0.004m.

Figure 4.10-4.12 showed that the velocity profile against Y when the leaflets are opened at different phase in pulsatile which are during acceleration, peak systole, and deceleration respectively. During acceleration, the case with VG yielded 1.20m/s at the centreline and 1.27m/s at peripheral. While the case without VG yielded 1.14m/s and 1.25m/s at peripheral. The differences of centre jet and peripheral jet between the case with VG and without VG are 0.06m/s (5.00%) and 0.02m/s (1.57%) respectively. During peak systole, the centre jet obtained by Co-rotating VG reached 1.46m/s while peripheral jet reached 1.49m/s. The differences at centre jet and peripheral jet are 0.06m/s (4.11%) and 0.03m/s (2.01%) respectively. In deceleration phase, the centre jet and peripheral jet velocities are 0.72m/s and 0.71m/s correspondingly. The differences are 0.04m/s (5.56%) and 0.02m/s (2.82%) at centreline and peripheral respectively. The velocity profile trends are the same in three different phase which are acceleration, peak systole and deceleration.

Co-rotating VG is generated vortices that aided streamline the flow and sustain at high velocity. It also maintained a more gradual decay at the leaflet’s tips at X = -0.004m. Without the installation of VG, the early separation is leaded to stronger turbulence, and more energy dissipation identified by a drastic drop in velocity along the prosthetic heart valve.

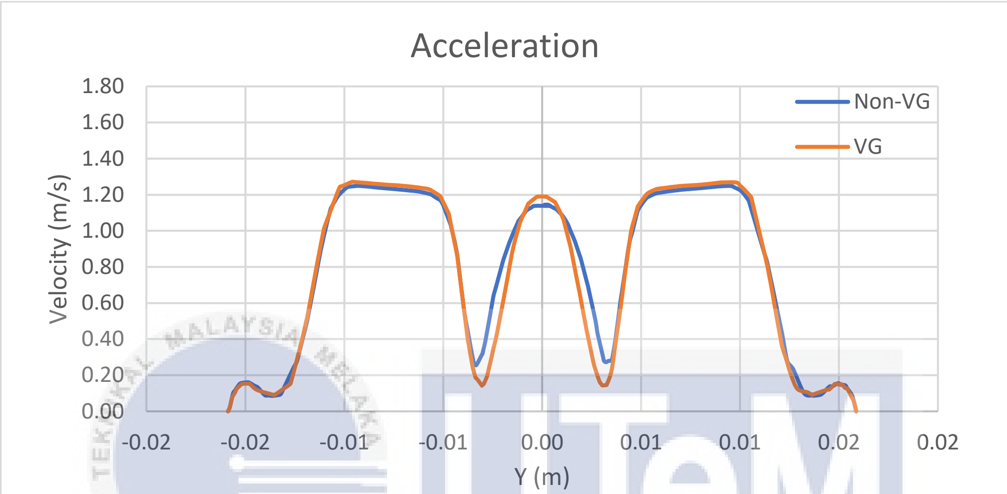

Figure 4.10: The Velocity Profile in Acceleration Stage.

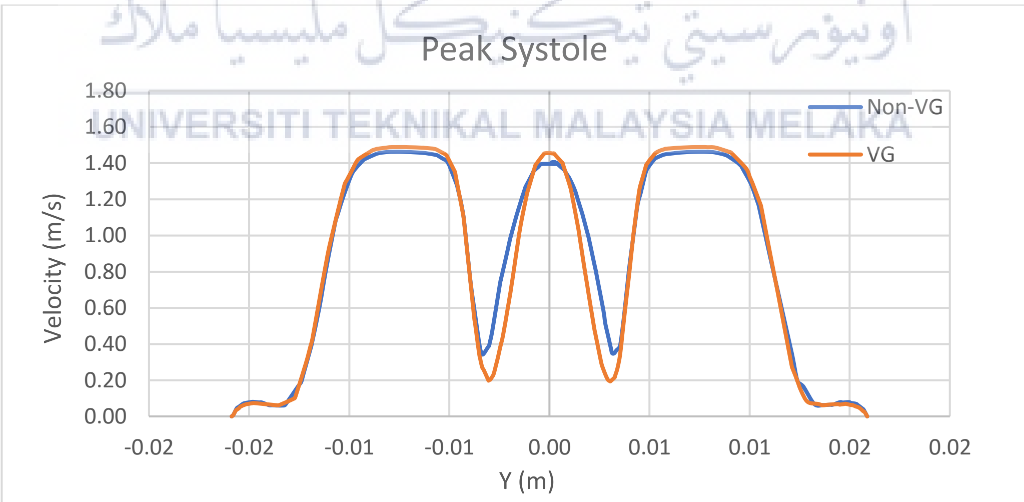

Figure 4.11: The Velocity Profile in Peak Systole Stage.

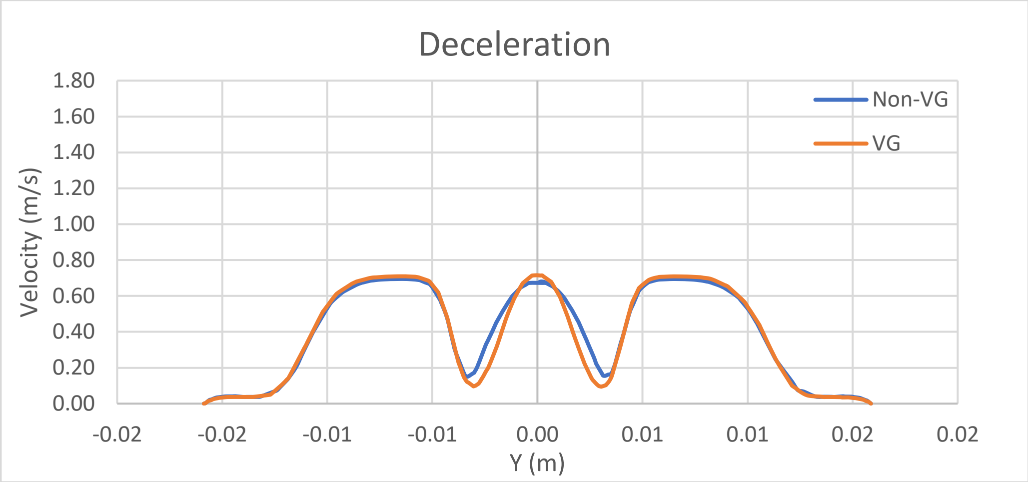

Figure 4.12: The Velocity Profile in Deceleration Stage.

CHAPTER 5

CONCLUSION AND RECOMMENDATION

In a mechanical heart valve, there are a lot of complications need to be improved. The formation of blood clotting is the most dangerous factor that caused a stroke. From the hemodynamic blood clot perspective, during the acceleration stage in pulsatile flow, the peak extrusion flow is generated a cavitation phenomenon. This will decrease the life cycle of a mechanical heart valve. Besides that, patients with mechanical heart valve need to inherit the risk associated with taking anticoagulation in the long term. The patients must be careful at all time. If he or she accidentally falls and making a wound, the blood bleeding cannot immediately stop, and they need to have a special treatment.

Due to the high shear stress and turbulent flow is generated in mechanical heart valve, the application of vortex generators is proposed to overcome the obstacles. Vortex generator is a device to reduce the flow separation and turbulent flow over a surface. The vortex generator is placed on the downstream flow of leaflets. The orientation of vortex generator is a key to manage the reduction of shear stress and turbulence. There are some criteria to determine the arrangements of vortex generators. Angle between VG blade and surface, curvilinear position of the line of vortex generator on the surface and spacing between vortex generator are the parameters used to decide the arrangements of vortex generator. It played a significant role to enhance the efficiency of mechanical heart valve.

The effectiveness of flow control concepts which is the installation of VG is applied to bi-leaflet prosthetic heart valve was evaluated and the most effective arrangement of VGs was identified among three model of arrangement. Co-rotating Equally Spaced VG is the most optimal arrangement of VG in this study. The addition of VG enhanced the pressure drop, TKE and turbulence shear stress compared to the case without any addition of VG. In summary, vortex generator is the most crucial device to enhance the performance of hemodynamic factor in mechanical prosthetic heart valve to mitigate the risk of formation of thrombus.

In this project, only three different of VG configurations were studied. Further studies are needed to investigate the geometry of VG, dimension of VG and orientation of VG to optimise the performance of VG in prosthetic heart valve.

REFERENCES

Aider, J. L., Beaudoin, J. F. and Wesfreid, J. E. (2010) 'Drag and lift reduction of a 3D bluff-body using active vortex generators', *Experiments in Fluids*, 48(5), pp. 771–789. doi: 10.1007/s00348-009-0770-y.

Akutsu, T. and Matsumoto, A. (2010) 'Influence of three mechanical bileaflet prosthetic valve designs on the three-dimensional flow field inside a simulated aorta', *Journal of Artificial Organs*, 13(4), pp. 207–217. doi: 10.1007/s10047-010-0519-7.

C, F. R. and Thiyagarajan, I. (2015) 'The Effect of Orientation of Vortex Generators on Aerodynamic Drag Reduction in Cars', 4(7), pp. 13–20.

Chou, C. C. *et al.* (2016) 'Decreased hemolysis and improved hemodynamic performance of synchronized bileaflet mechanical valve', *Annals of Thoracic Surgery*. The Society of Thoracic Surgeons, 101(3), pp. 1153–1158. doi: 10.1016/j.athoracsur.2015.10.111.

Ge, L. *et al.* (2003) 'Numerical Simulation of Flow in Mechanical Heart Valves: Grid Resolution and the Assumption of Flow Symmetry', *Journal of Biomechanical Engineering*, 125(5), pp. 709–718. doi: 10.1115/1.1614817.

Hassan, S. M. R. *et al.* (2014) 'Numerical Study on Aerodynamic Drag Reduction of Racing Cars', *Procedia Engineering*. Elsevier B.V., 90, pp. 308–313. doi: 10.1016/j.proeng.2014.11.854.

Hatoum, H. *et al.* (2018) 'An in vitro evaluation of turbulence after transcatheter aortic valve implantation', *Journal of Thoracic and Cardiovascular Surgery*. Elsevier Inc., 156(5), pp. 1837–1848. doi: 10.1016/j.jtcvs.2018.05.042.

Hatoum, H. and Dasi, L. P. (2019) 'Reduction of Pressure Gradient and Turbulence Using Vortex Generators in Prosthetic Heart Valves', *Annals of Biomedical Engineering*, 47(1), pp. 85–96. doi: 10.1007/s10439-018-02128-6.

Hedayat, M., Asgharzadeh, H. and Borazjani, I. (2017) 'Platelet activation of mechanical versus bioprosthetic heart valves during systole', *Journal of Biomechanics*. Elsevier, 56, pp. 111–116. doi: 10.1016/J.JBIOMECH.2017.03.002.

Ischemic Heart Disease | National Heart, Lung, and Blood Institute (NHLBI) (no date). Available at: https://www.nhlbi.nih.gov/health-topics/ischemic-heart-disease (Accessed: 24 November 2019).

James, M. E., Papavassiliou, D. V. and O'Rear, E. A. (2019) 'Use of computational fluid dynamics to analyze blood flow, hemolysis and sublethal damage to red blood cells in a bileaflet artificial heart valve', *Fluids*, 4(1). doi: 10.3390/fluids4010019.

Li, K. Y. C. (2019) 'Bioprosthetic Heart Valves: Upgrading a 50-Year Old Technology', *Frontiers in Cardiovascular Medicine*, 6(April), pp. 1–6. doi: 10.3389/fcvm.2019.00047.

Mohammadi, H., Jahandardoost, M. and Fradet, G. (2015) 'Elliptic st. jude bileaflet mechanical heart valves', *Cardiovascular System*, 3(1), p. 1. doi: 10.7243/2052-4358-3-1.

Pibarot, P. and Dumesnil, J. G. (2009) 'Prosthetic heart valves: Selection of the optimal prosthesis and long-term management', *Circulation*, 119(7), pp. 1034–1048. doi: 10.1161/CIRCULATIONAHA.108.778886.

Ponikowski, P. *et al.* (2014) 'Heart failure: preventing disease and death worldwide', *ESC Heart Failure*, 1(1), pp. 4–25. doi: 10.1002/ehf2.12005.

Raser, K. A. H. F. *et al.* (2008) 'Characterization of an Abdominal Aortic Velocity Waveform in Patients with Abdominal Aortic Aneurysm CHARACTERIZATION OF AN ABDOMINAL AORTIC VELOCITY WAVEFORM IN PATIENTS WITH ABDOMINAL AORTIC ANEURYSM', (February). doi: 10.1016/j.ultrasmedbio.2007.06.015.

Salleh, N. M. *et al.* (2020) 'Reducing of Thrombosis in Mechanical Heart Valve through the Computational Method : A Review', 2(2), pp. 178–200.

Sotiropoulos, F., Le, T. B. and Gilmanov, A. (2016) 'Fluid Mechanics of Heart Valves and Their Replacements', *Annual Review of Fluid Mechanics*, 48(1), pp. 259–283. doi: 10.1146/annurev-fluid-122414-034314.

Wang, H. *et al.* (2017) 'Flow control on the NREL S809 wind turbine airfoil using vortex generators', *Energy*. Elsevier Ltd, 118, pp. 1210–1221. doi: 10.1016/j.energy.2016.11.003.

Yun, B. M., Dasi, L. P., *et al.* (2014) 'Computational modelling of flow through prosthetic heart valves using the entropic lattice-Boltzmann method', *Journal of Fluid Mechanics*, 743, pp. 170–201. doi: 10.1017/jfm.2014.54.

Yun, B. M., McElhinney, D. B., *et al.* (2014) ‘Computational simulations of flow dynamics and blood damage through a bileaflet mechanical heart valve scaled to pediatric size and flow’, *Journal of Biomechanics*. Elsevier, 47(12), pp. 3169–3177. doi: 10.1016/J.JBIOMECH.2014.06.018.

Zakaria, M. S. *et al.* (2017) ‘Review of numerical methods for simulation of mechanical heart valves and the potential for blood clotting’, *Medical and Biological Engineering and Computing*. Springer Berlin Heidelberg, 55(9), pp. 1519–1548. doi: 10.1007/s11517-017-1688-9.

Zakerzadeh, R., Hsu, M. C. and Sacks, M. S. (2017) ‘Computational methods for the aortic heart valve and its replacements’, *Expert Review of Medical Devices*. Taylor & Francis, 14(11), pp. 849–866. doi: 10.1080/17434440.2017.1389274.

Zbavitel, J. and Fialová, S. (2019) ‘A numerical study of hemodynamic effects on the bileaflet mechanical heart valve’, *EPJ Web of Conferences*, 213, p. 02103. doi: 10.1051/epjconf/201921302103.

Zhang, L. *et al.* (2016) ‘Effects of vortex generators on aerodynamic performance of thick wind turbine airfoils’, *Journal of Wind Engineering and Industrial Aerodynamics*. Elsevier, 156, pp. 84–92. doi: 10.1016/j.jweia.2016.07.013.